



LASER ATMOSPHERIC ABSORPTION STUDIES

R. K. Long
E. K. Damon
R. J. Nordstrom
J. C. Peterson
M. E. Thomas
J. Sherman

The Ohio State University

ElectroScience Laboratory

Department of Electrical Engineering
Columbus, Ohio 43212

Interim Report 4232-4

May 1977

Contract F30602-76-C-0058

Approved for public release; distribution unlimited.

Sponsored by
Defense Advanced Research Projects Agency (DoD)
ARPA Order No. 1279

The views and conclusions contained in this document are those of the authors and should not be interpreted as necessarily representing the official policies, either expressed or implied, of the Defense Advanced Research Projects Agency or the U. S. Government.

ROME AIR DEVELOPMENT CENTER
AIR FORCE SYSTEMS COMMAND
GRIFFISS AIR FORCE BASE, NEW YORK 13441

PLEASE RETURN TO:
BMD TECHNICAL INFORMATION CENTER
BALLISTIC MISSILE DEFENSE ORGANIZATION
7100 DEFENSE PENTAGON
WASHINGTON D.C. 20301-7100

19980513 107

DTIC QUALITY INSPECTED

U3789

NOTICES

When Government drawings, specifications, or other data are used for any purpose other than in connection with a definitely related Government procurement operation, the United States Government thereby incurs no responsibility nor any obligation whatsoever, and the fact that the Government may have formulated, furnished, or in any way supplied the said drawings, specifications, or other data, is not to be regarded by implication or otherwise as in any manner licensing the holder or any other person or corporation, or conveying any rights or permission to manufacture, use, or sell any patented invention that may in any way be related thereto.

Accession Number: 3789

Publication Date: May 01, 1977

Title: Laser Atmospheric Absorption Studies

Personal Author: Long, R.K.; Damon, E.K.; Nordstrom, R.J. et al.

Corporate Author Or Publisher: Ohio State University ElectroScience Lab, Columbus, OH 43212 Report Number: RADC-TR-77

Report Prepared for: Rome Air Development Center (OCSE), Griffiss AFB, NY 13441 Report Number Assigned by Contract Monitor: SLL 78-058/P/P

Comments on Document: Archive, RRI, DEW

Descriptors, Keywords: Directed Energy Weapon DEW Molecular Absorption Laser Propagation CO2 CO Spectrophone White Cell Long-path Multi-pass H2O

Pages: 00056

Cataloged Date: Oct 19, 1992

Contract Number: F30602-76-C-0058

Document Type: HC

Number of Copies In Library: 000001

Record ID: 24954

Source of Document: DEW

REPORT DOCUMENTATION PAGE		READ INSTRUCTIONS BEFORE COMPLETING FORM
1. REPORT NUMBER RADC-TR-77-	2. GOVT ACCESSION NO.	3. RECIPIENT'S CATALOG NUMBER
4. TITLE (and Subtitle) LASER ATMOSPHERIC ABSORPTION STUDIES		5. TYPE OF REPORT & PERIOD COVERED Interim Report Jul 76 - May 77
		6. PERFORMING ORG. REPORT NUMBER ESL 4232-4
7. AUTHOR(s) R. K. Long J. C. Peterson E. K. Damon M. E. Thomas R. J. Nordstrom J. Sherman		8. CONTRACT OR GRANT NUMBER(s) F30602-76-C-0058
9. PERFORMING ORGANIZATION NAME AND ADDRESS The Ohio State University ElectroScience Laboratory, Department of Electrical Engineering Columbus OH 43212		10. PROGRAM ELEMENT, PROJECT, TASK AREA & WORK UNIT NUMBERS 62301E 12790508
11. CONTROLLING OFFICE NAME AND ADDRESS Defense Advanced Research Projects Agency 1400 Wilson Blvd Arlington VA 22209		12. REPORT DATE May 1977
		13. NUMBER OF PAGES 57
14. MONITORING AGENCY NAME & ADDRESS (if different from Controlling Office) Rome Air Development Center (OCSE) Griffiss AFB NY 13441		15. SECURITY CLASS. (of this report) UNCLASSIFIED
		15a. DECLASSIFICATION/DOWNGRADING SCHEDULE N/A
16. DISTRIBUTION STATEMENT (of this Report) Approved for public release; distribution unlimited		
17. DISTRIBUTION STATEMENT (of the abstract entered in Block 20, if different from Report) Same		
18. SUPPLEMENTARY NOTES RADC Project Engineer: James W. Cusack (OCSE)		
19. KEY WORDS (Continue on reverse side if necessary and identify by block number) Molecular absorption Spectrophone CO ₂ Laser White cell H ₂ O Laser propagation Long-path cell CO ₂ laser Multi-pass cell CO laser		
20. ABSTRACT (Continue on reverse side if necessary and identify by block number) This report describes progress on the various tasks which comprise the research in laser atmospheric propagation. This work includes 1. a review of work done on the study of the infrared water vapor continuum, 2. the design of low stainless steel, temperature controlled absorption cells with White-type optics, 3. design of a non-resonant, differential spectrophone and data recorded on this instrument, 4. design of a stainless steel, resonant spectrophone, 5. and other topics.		

LASER ATMOSPHERIC ABSORPTION STUDIES

R. K. Long
E. K. Damon
R. J. Nordstrom
J. C. Peterson
M. E. Thomas
J. Sherman

Contractor: The Ohio State University
Contract Number: F30602-76-C-0058
Effective Date of Contract: 1 July 1975
Contract Expiration Date: 30 September 1977
Short Title of Work: Laser Atmospheric
Absorption Studies
Program Code Number: 6E20
Period of Work Covered: Jul 76 - May 77
Principal Investigator: Dr. Ronald K. Long
Phone : 614 422-6077
Project Engineer: James W. Cusack
Phone : 315 330-3145

Approved for public release;
distribution unlimited.

This research was supported by the Defense Advanced
Research Projects Agency of the Department of
Defense and was monitored by James W. Cusack (OCSE),
Griffiss AFB NY 13441 under Contract F30602-76-C-0058.

CONTENTS

	Page
I. SPECTROPHONE STUDIES	1
II. WHITE CELL CONSTRUCTION	10
III. CO LASER TRANSMITTANCE - CALCULATION AND MEASUREMENT	11
A. Introduction	11
B. Calculations	11
C. Measurements	11
IV. ISOTOPE CO ₂ LASER TRANSMITTANCE CALCULATIONS	42
V. OZONE SPECTROSCOPY NEAR 5 μm	46
VI. MISCELLANEOUS TOPICS	50
A. Modification of Commercial CO ₂ Laser	50
B. CW HF/DF Laser System	53
C. Microcomputer Data Link	55
D. Fourier Transform Spectrometer	55
REFERENCES	56

SECTION I

SPECTROPHONE STUDIES

One of the most important problems in experimental linear absorption spectroscopy is to measure the temperature dependence of absorption coefficients, especially the water vapor continuum where theoretical uncertainty exists.

The stainless steel spectrophone has been employed for the first time to make 10 μm water vapor and CO_2 absorption coefficient measurements as a function of temperature. Preliminary results indicate that the instrument will be capable of producing accurate and repeatable temperature data as soon as a few minor problems are resolved. At this time, calibration of the spectrophone is the only serious unresolved problem. The other difficulties, which will be described below, have been eliminated or are in the process of being corrected.

The first major problem encountered with the spectrophone was an unacceptable level of noise in the output of the BARATRON (M.K.S. trademark) pressure transducer. This instrument was returned to the factory for testing and repair after our initial efforts to correct this problem were unsuccessful. After several months of testing the manufacturer has agreed to replace the complete unit with one not having this problem. Apparently the noise was caused by an interaction between the pressure head bridge - preamplifier circuits and the output electronics which could not be traced to a single source.

In order to continue making measurements (while the BARATRON was serviced) a BAROCEL (Datametrics trademark) electronic manometer originally used on the aluminum spectrophone was connected to the s.s. spectrophone. This did not result in an optimum system since the spectrophone and the spacing and length of certain tubing had been designed for the particular model of BARATRON. Nevertheless, we were able to perform a number of measurements and tests on the spectrophone during this time. These tests have indicated that the background window signal caused by absorption and/or scattering of the laser radiation was greatest in the long cell of the differential spectrophone. By switching the end windows (from the long to the short chamber and vice versa) it was demonstrated that the window originally on the long cell was in some way inferior and responsible for a higher background signal. This problem is currently being studied.

Modifications to the spectrophone laboratory have also been made to reduce mechanical sources of noise. The optical table has been mounted on a vibration isolation mount to prevent vibration in the floor from being transmitted to the experimental apparatus on the table. Also, all the mechanical vacuum pumps have been removed from the laboratory.

This required the installation of three 2" vacuum lines from spectrophone lab to the back of the main laboratory, where the pumps are now located.

The first measurements performed with water vapor indicated that two significant and undesirable effects were being observed. The first effect caused the level of absorption to be greater than that which was expected and to increase with time as the sample remained in the instrument. This was attributed to contaminants on the walls of the spectrophone plumbing and the gas handling system. The problem was eliminated by re-cleaning all tubing, fittings, valves and the spectrophone with carbon tetrachloride in an ultrasonic cleaner and then boiling these parts in double distilled water for an hour. This cleaning procedure seems to have solved the contamination problem. Water vapor samples have been circulated in the current spectrophone plumbing system for as long as 80 minutes without any increase in absorption.

The second problem also caused the absorption to be higher than expected but it was caused by an entirely different problem. Until this difficulty was resolved the spectrophone data indicated an anomalous increase in absorption for samples with relative humidities of 50% or higher. Ultimately this was traced to the method by which samples were being introduced and mixed. This improper method resulted in an incompletely mixed sample with a significantly higher (than average) concentration of H₂O near the ends of the spectrophone. An example of this type of response is shown in Figure 1. A proper sample handling and mixing procedure has eliminated the problem.

Results of water vapor measurements performed on the 10 μ m P(20) and R(20) lines are given in Figures 2 and 3 respectively. This data is given in terms of the raw experimental values of S/W, i.e., the ratio of the pressure signal divided by the laser power. (The approximate level of absorption can be obtained by multiplying this ratio by the calibration constant 0.25 [$\text{km}^{-1}/(\text{S}/\text{W})$]). A reliable and accurate calibration of the spectrophone has not yet been determined so that we have supplied only the raw data. The next step to be completed will be determining an accurate calibration for the spectrophone.

The data for the P(20) and R(20) lines indicates several interesting aspects of the temperature dependence of water vapor absorption. One significant fact is that absorption at the P(20) line shows a negative temperature coefficient while that for the R(20) line is positive. This difference which was expected can be explained by the fact that the P(20) line is removed from any local lines while the R(20) line is located within the half width of a strong local water vapor line. This data also indicates that the effects of temperature on water vapor absorption are quite significant and can be easily observed with small changes in the spectrophone temperature.

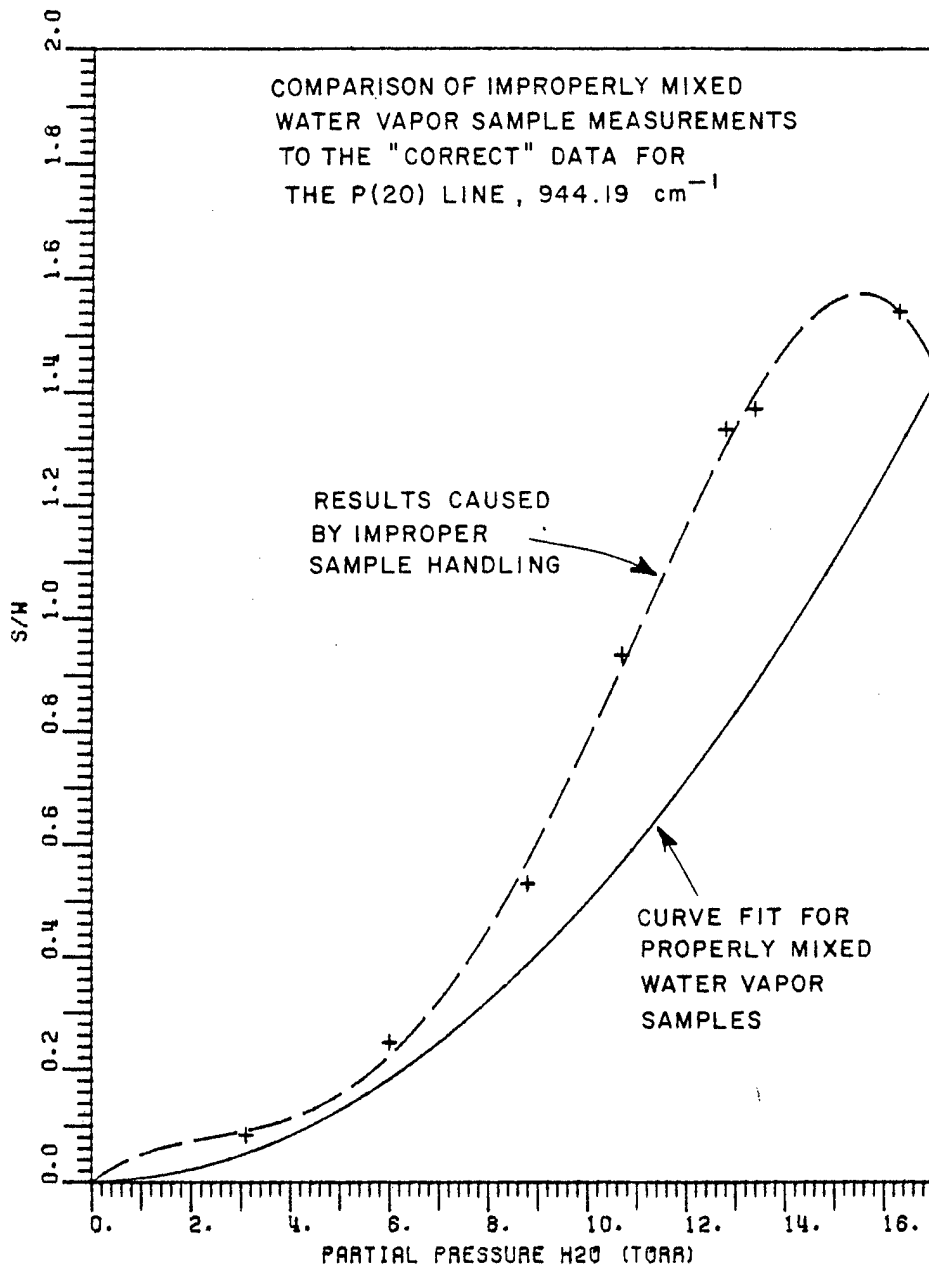


Figure 1. An illustration of the problems caused by incomplete sample mixing in the spectrophone.

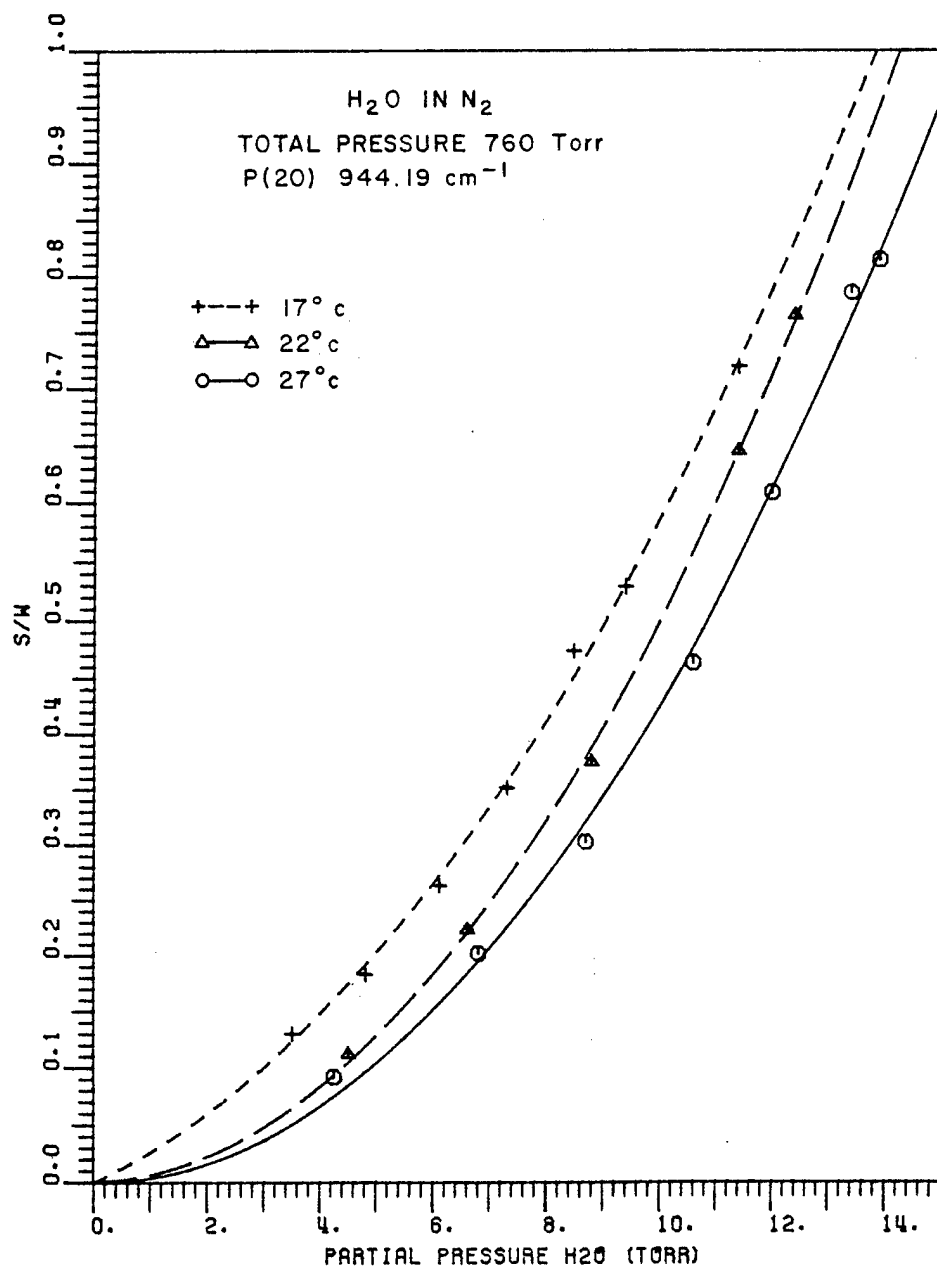


Figure 2. Spectrophone measurements of relative absorption coefficient for water vapor at 944.194 cm⁻¹ for three temperatures.

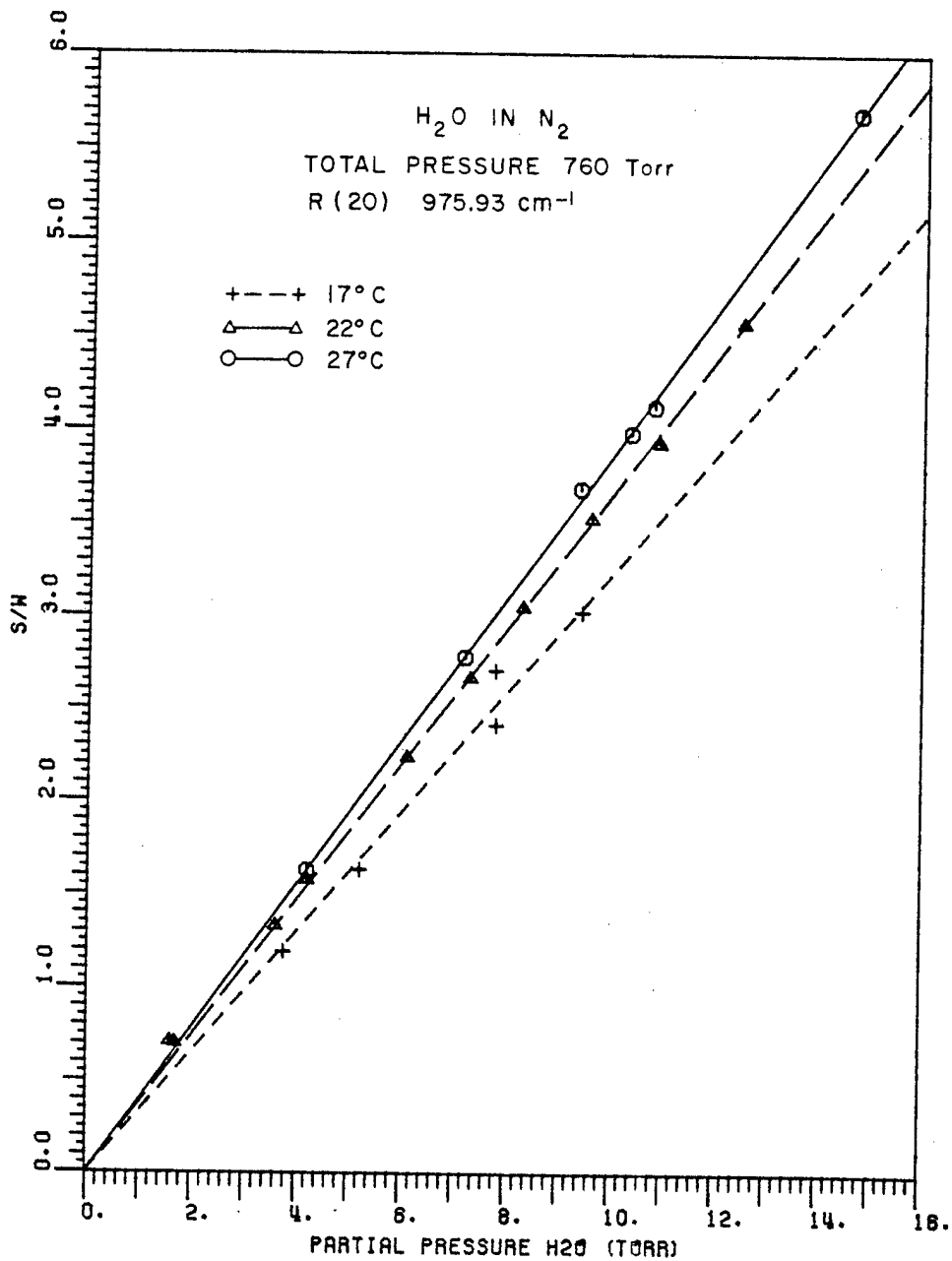


Figure 3. Spectrophone measurements of relative absorption coefficients for water vapor broadened with N_2 to 760 Torr at 975.93 cm^{-1} for three temperatures.

Calibration of the spectrophone requires that accurate White cell data be obtained at a known temperature, T_0 . Previous White cell measurements were performed without adequate documentation of the temperature. Once this White cell data has been determined the spectrophone can be calibrated by performing a spectrophone measurement on an identical sample of gas at this same temperature, T_0 . Compensation for the effects of temperature on instrument response appears at this stage to be a rather simple process. From the theory of spectrophones it is known that the instrument response, S (the pressure signal) is related to the absorption coefficient, α of the sample gas by the expression

$$\frac{S}{W} = C_0 \frac{\alpha}{T} \quad (1)$$

where

W = laser power
 T = absolute temperature
 C_0 = a constant factor.

Assuming from White cell results that $\alpha = \alpha_0$ is known for a given sample concentration at a temperature T_0 we then measure (S/W) to obtain a calibration constant, i.e.,

$$(S/W)^0 = \frac{C_0}{T_0} \alpha^0 = \theta_0 \alpha^0, \text{ where } \theta_0 = \frac{C_0}{T_0} . \quad (2)$$

Hence, θ_0 can be determined and is the calibration constant. When performing measurements at any other temperature, T_1

$$(S/W)^1 = \frac{C_0}{T_1} \alpha' = \frac{C_0}{T_0} \alpha' \frac{T_0}{T_1} = \theta_0 \alpha' \frac{T_0}{T_1} . \quad (3)$$

So that the absorption coefficient, for a sample at temperature T_1 can be determined from the calibration coefficient measured at temperature T_0 by simply scaling the results by the ratio of the two temperatures, i.e.,

$$\alpha' = \frac{(S/W)^1}{\theta_0} \frac{T_1}{T_0} . \quad (4)$$

Note that this correction has not been applied to the data of Figures 2 and 3. This is intended to be part of the data reduction when a better value for θ_0 is determined.

An analysis of the spectrophone temperature data has not been completed and will not be seriously undertaken until the recalibration of the instrument is completed. The reasonableness of the relative data can be confirmed by comparing with AFGL line listing calculations for

a case where the fundamental processes are more or less known, vis-a-vis the water continuum for example.

Figure 4 shows measurements of the relative absorption of carbon dioxide, broadened with nitrogen to 760 Torr, at the 944.194 cm^{-1} P(20) laser line for three temperatures. The absolute value of the experimental data is not known but a percentage change can be calculated and compared with theoretical prediction. When the S/W values are corrected by T/T_0 the average change per deg C is 2.43 percent compared to 2.1 percent computed from the line data tape.

Figure 5 shows similar carbon dioxide absorption data for the R(20) laser line at 975.931 cm^{-1} . Here the average change is 2.33 percent per degree compared to a calculated value of 2.1 percent.

Figure 2 gives measurements of absorption by water vapor, broadened to 760 Torr by nitrogen, at the 944.194 cm^{-1} P(20) laser line for three temperatures. For this case it is necessary to include a continuum contribution to the calculated coefficient. The method used for this is described in connection with another topic in Chapter IV of this report, see Equation (7). Since the absorption is non-linear, a comparison at two partial pressures of water vapor is made. When the 17 C and 27 C data are used, the 10 Torr case yields a measured coefficient of 2.6 percent per deg C compared to a calculated value of 2.1 percent, whereas for 14.3 torr the experimental value is 1.3 percent compared to a calculated 1.4 percent. A comparison at 5 Torr was also made with less satisfactory results but the experimenter feels that the experimental error may be higher for that case.

An attempt was also made to analyze the R(20) water vapor data of Figure 3. For this case the absorption is dominated by a single close water line and the computed change with temperature will depend on the frequency of the laser line with respect to the water line in the AFGL listing. A previous experiment using a White cell which measured absorption vs total pressure determined a separation of 0.025 cm^{-1} between laser and water line. If this is incorporated into the calculation by using an appropriate "laser frequency", the calculation at 14.3 Torr gives 1.8 percent per deg C compared to a measurement of 2.4 percent per deg C.

The above should be classed as preliminary comments. When more data is available a more complete analysis will be possible. However it has been shown that a spectrophone can be used to collect precision data on temperature effects. The technique holds much promise for the future.

Future work will include efforts to study the temperature dependence of water vapor and CO_2 absorption for a significant number of CO_2 lines in the 9 and 10 μm bands. Efforts will be made to connect these results with existing theories for the temperature dependence of H_2O and CO_2 absorption. It is also expected that a wider range in temperatures than that demonstrated here will be employed in this study.

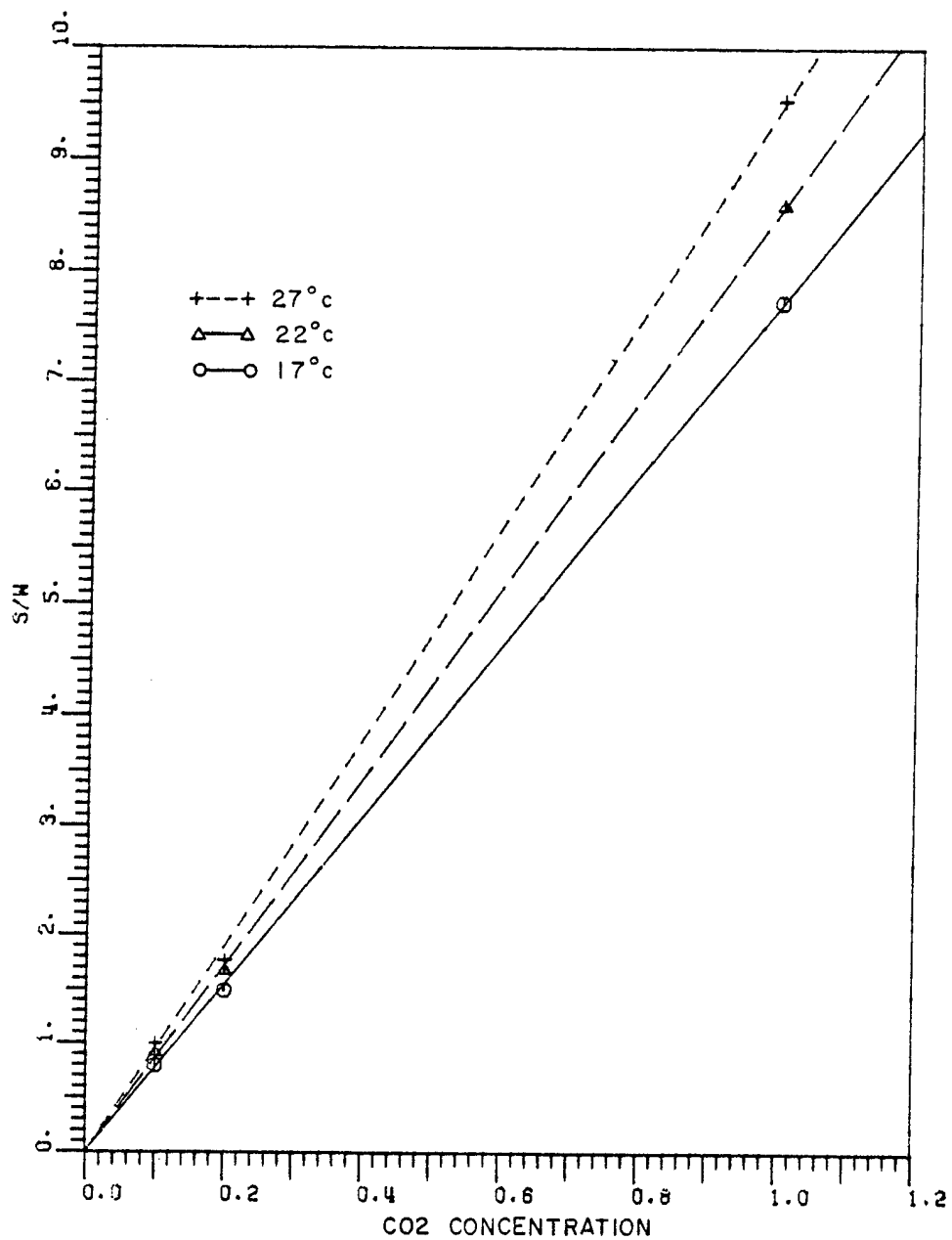


Figure 4. Spectrophone measurements of relative absorption coefficient for CO₂ broadened with N₂ to 760 Torr at 944.194 cm⁻¹ for three temperatures.

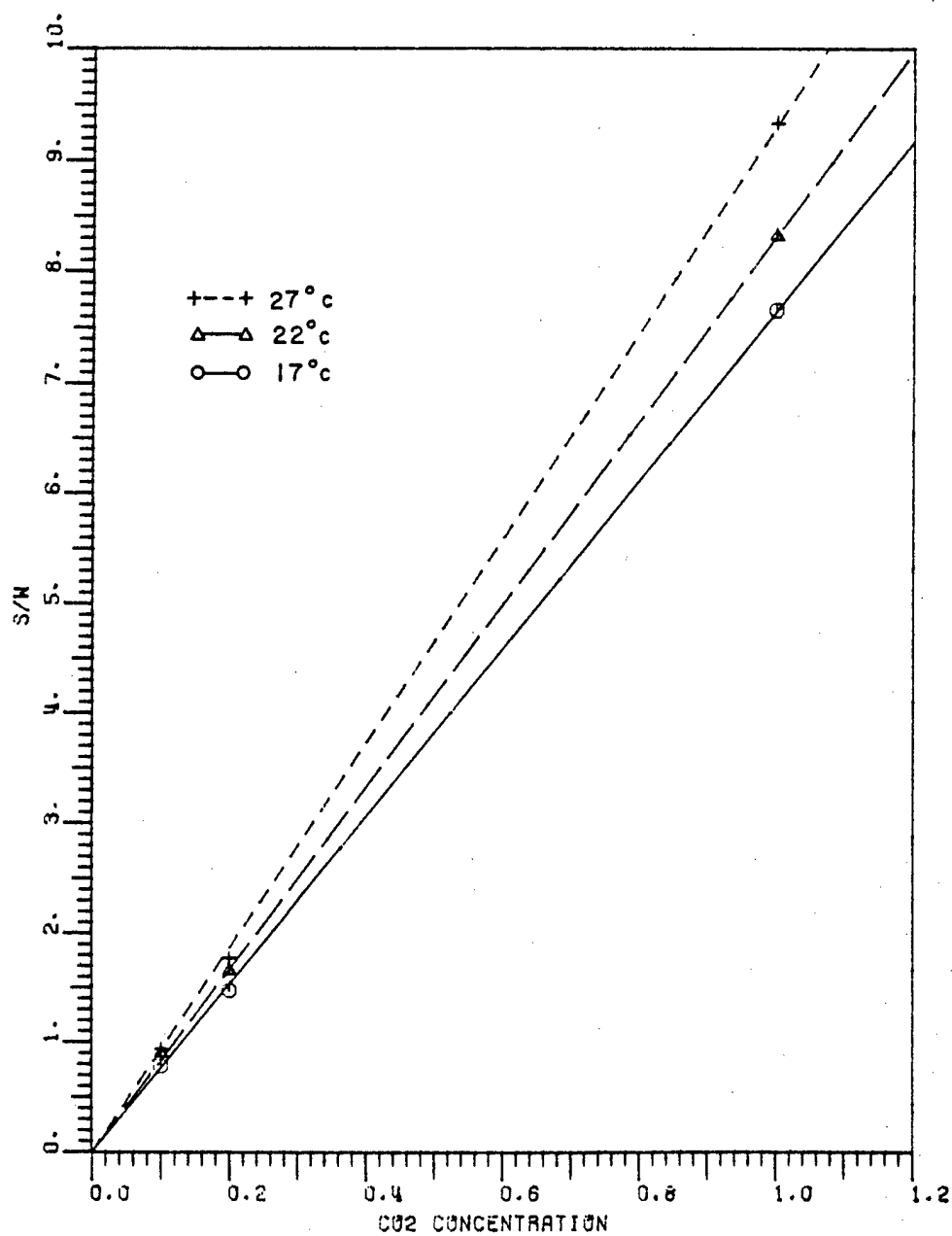


Figure 5. Spectrophone measurements of relative absorption coefficient for CO₂ broadened with N₂ to 760 Torr at 975.93 cm⁻¹ for three temperatures.

SECTION II

WHITE CELL CONSTRUCTION

The design philosophy of the new multi-pass absorption cell was documented in a previous report [1]. Briefly, the vacuum chamber is 40 feet long and 24 inches in diameter. Mirror spacing is 10.785 meters (35.4 feet) with multi-pass capability to at least one km. The system is stainless steel, and can be temperature controlled between -60 C and +60 C. Photographs of the vacuum chamber and the optical mounts were shown in a subsequent report [2].

The temperature control system and connections to the cell have been completed and testing has begun, although full temperature testing must await installation of the insulating jacket.

The diffusion pump and its manifold have been constructed and installed. The main mechanical roughing pump had failed in other service, and is being repaired. With a smaller roughing pump, vacuum integrity of the chamber (without optics) was tested, and a vacuum of 5×10^{-6} Torr achieved after repairing several minor leaks. This is about the level expected if oil contamination is present, which could take months of outgassing to eliminate. Since the cell has not been cleaned, it was shut down, the interior welds were smoothed further and the cell and pumps cleaned with detergent and then alcohol. It is currently ready to reassemble and test.

The main optics mounts have been assembled and tested with their stepper motor drives, and appear to operate as expected. The stepper drives and associated housings have been vacuum checked. The entrance and exit periscopes and the path doubling roof mirror mounts are under construction. This last phase had been delayed until the optics of the Fourier transform spectrometer were established to assure full compatibility. Entrance and exit optics to match the cell to the FTS and detector have been designed.

Auxiliary systems such as sample handling, gauging, and related equipment is in various stages of construction or test. A distribution manifold which will introduce the nitrogen or air broadening gas into the cell at 42 different points simultaneously has been constructed, and should alleviate mixing problems commonly associated with large cells.

In the near future we will: (1) vacuum check the cleaned system, (2) install insulation, and (3) install the optics and conduct a full system checkout.

SECTION III
CO LASER TRANSMITTANCE - CALCULATION AND MEASUREMENT

A. Introduction

This section presents calculations and experimental measurements (water vapor only) of atmospheric transmittance for CO laser frequencies.

B. Calculations

Previous publications [3,4] dealing with CO laser transmittances based on the AFGL data tape are inadequate or in need of updating.

The calculations given here have the following features:

- a. The latest AFGL tape (September 1976) is used.
- b. CO laser frequencies of improved accuracy are used [5].
- c. The absorption coefficient is listed for each absorbing species separately which some codes require.
- d. A super-Lorentz line shape is used for water vapor.
- e. A Voigt profile is used for lower pressures.

The basic calculation technique has been described previously [6]. It has been shown [7] that a super-Lorentz line shape for water vapor improves the agreement at sea level between experiment and prediction. With respect to the ozone coefficients it should be noted that some combination bands of ozone in this spectral region are not included in the AFGL listing. Another part of this program (see Chapter V) involves the collection of new spectra of ozone in this region. Results thus far obtained are not complete enough to impact these calculations, however.

Calculations have been performed for the P(15) to P(1) line of the 8-7 to 3-2 CO bands. The AFGL mid-latitude summer model has been used throughout. Program parameters such as broadening coefficients etc. are the same as in previous OSU reports [6]. The absorption coefficients given in Figures 6 to 29 are in km^{-1} for the altitudes shown from 0 to 50 km.

C. Experimental Measurements in Water Vapor

Experimental measurements of water vapor transmittance have been performed using N_2 buffer gas at 760 Torr total pressure and a temperature near 23 C. A cw CO laser source was used with a multipass cell having lengths of up to 1.1 km.

The data are in two groups:

- a. A group of measurements for 11 CO lines which is a re-interpretation of previous data measured at OSU [7] in 1973.
- b. Data for 4 CO lines which was obtained during the present period. Two of these lines are duplicates of the 1973 measurements permitting a comparison of experiments; the absorption cell is the same but the laser and all other components are different. The remaining lines are in the 4-3 band which could not be studied with the laser used in 1973.

With respect to the first group, the data is republished here with a straight line fit instead of the quadratic fit used previously. The scatter in the experimental data is such that, especially for the most highly transmitting lines, the second order term is not meaningful. For some cases such as the 6-5 P(14) line (see below) the non-linear behavior has been confirmed, however.

With the availability of a new liquid nitrogen cooled CO laser which has output on lines of the 2-1, 3-2 and 4-3 bands which were not available from the laser used in 1973, a new series of water vapor absorption measurements was planned. The results of the first four lines studied are presented here in Figures 33a-d.

Figure 33a shows the 6-5 P(14) line which is also given in Figure 31d and in Reference 7. The laser line is very near a local water line which accounts for the negative curvature. Improved techniques have reduced the data scatter over the earlier measurement. These include the use of a visible laser (argon) to continuously monitor the White cell alignment and correction of alignment when required, and mechanical modifications which have reduced vibrations of the cell caused by vacuum pumps and mixing fans. In general the greatest difficulty has been long term drift caused by optical alignment problems. We hope that the new cell, see Section II will be much better in this respect.

Figure 33b shows the 5-4 P(15) line which is also a repeat of a line studied earlier. This was the highest transmittance line in the 1973 study. Good agreement has been obtained with the 1973 results. Because of the improved techniques noted above and the longer path length used in the current study the present results are considered to be more accurate.

Figure 33c and 33d show data for new lines, 4-3 P(13) and 4-3 P(10). In both cases the data scatter is quite small. These lines transmit as well as the best line of the earlier study, i.e., 5-4 P(15).

In the next quarter these measurements will be extended to cover all of the 4-3 and 3-2 band lines obtainable from our laser, see Reference 2 page 41. We are also coordinating our program with the outdoor measurements by NRL at Cape Canaveral so that a laboratory-outdoor comparison can be made.

DATE 03/04/77 1935.4266
LASER LINE 1944.7448
MODEL: MID-LATITUDE SUMMER
MALTAEZ 3.000, FTAZ 1.770

ALT.	0	1	2	3	4	5	6	7	8
0.0	1.420	0	0	0	0	0	0	0	0
1.0	9.596	1	5.982	2	0.000	0	0.000	1	1.666
2.0	5.797	0	5.134	2	0.000	0	0.000	0	2.890
3.0	4.430	0	4.430	3	0.000	0	0.000	0	2.430
4.0	3.535	0	3.535	4	0.000	0	0.000	0	2.175
5.0	2.958	0	2.958	5	0.000	0	0.000	0	1.976
6.0	2.595	0	2.595	6	0.000	0	0.000	0	1.811
7.0	2.330	0	2.330	7	0.000	0	0.000	0	1.686
8.0	2.116	0	2.116	8	0.000	0	0.000	0	1.598
9.0	1.945	0	1.945	9	0.000	0	0.000	0	1.537
10.0	1.813	0	1.813	10	0.000	0	0.000	0	1.497
11.0	1.713	0	1.713	11	0.000	0	0.000	0	1.471
12.0	1.639	0	1.639	12	0.000	0	0.000	0	1.456
13.0	1.587	0	1.587	13	0.000	0	0.000	0	1.450
14.0	1.551	0	1.551	14	0.000	0	0.000	0	1.450
15.0	1.527	0	1.527	15	0.000	0	0.000	0	1.457
16.0	1.511	0	1.511	16	0.000	0	0.000	0	1.468
17.0	1.501	0	1.501	17	0.000	0	0.000	0	1.480
18.0	1.495	0	1.495	18	0.000	0	0.000	0	1.493
19.0	1.493	0	1.493	19	0.000	0	0.000	0	1.506
20.0	1.495	0	1.495	20	0.000	0	0.000	0	1.519
21.0	1.499	0	1.499	21	0.000	0	0.000	0	1.532
22.0	1.505	0	1.505	22	0.000	0	0.000	0	1.545
23.0	1.512	0	1.512	23	0.000	0	0.000	0	1.558
24.0	1.520	0	1.520	24	0.000	0	0.000	0	1.571
25.0	1.528	0	1.528	25	0.000	0	0.000	0	1.584
30.0	1.600	0	1.600	30	0.000	0	0.000	0	1.668
35.0	1.741	0	1.741	35	0.000	0	0.000	0	1.814
40.0	1.945	0	1.945	40	0.000	0	0.000	0	2.020
45.0	2.204	0	2.204	45	0.000	0	0.000	0	2.280
50.0	2.522	0	2.522	50	0.000	0	0.000	0	2.605

DATE 03/04/77 1944.7448
LASER LINE 1944.7448
MODEL: MID-LATITUDE SUMMER
MALTAEZ 3.000, FTAZ 1.770

ALT.	0	1	2	3	4	5	6	7	8
0.0	1.549	1	8.222	4	0.000	0	0.000	0	0.000
1.0	6.975	0	7.111	4	0.000	0	0.000	0	5.978
2.0	4.968	0	6.098	4	0.000	0	0.000	0	4.740
3.0	3.702	0	5.127	4	0.000	0	0.000	0	3.815
4.0	2.911	0	4.315	4	0.000	0	0.000	0	3.211
5.0	2.511	1	3.601	4	0.000	0	0.000	0	2.811
6.0	2.261	1	2.978	4	0.000	0	0.000	0	2.561
7.0	2.111	1	2.638	4	0.000	0	0.000	0	2.411
8.0	2.011	2	2.451	4	0.000	0	0.000	0	2.311
9.0	1.961	2	2.341	4	0.000	0	0.000	0	2.261
10.0	1.931	3	2.271	4	0.000	0	0.000	0	2.231
11.0	1.911	3	2.231	4	0.000	0	0.000	0	2.211
12.0	1.891	4	2.211	4	0.000	0	0.000	0	2.201
13.0	1.881	4	2.201	4	0.000	0	0.000	0	2.201
14.0	1.871	5	2.191	4	0.000	0	0.000	0	2.201
15.0	1.861	5	2.181	4	0.000	0	0.000	0	2.201
16.0	1.851	6	2.171	4	0.000	0	0.000	0	2.201
17.0	1.841	6	2.161	4	0.000	0	0.000	0	2.201
18.0	1.831	7	2.151	4	0.000	0	0.000	0	2.201
19.0	1.821	7	2.141	4	0.000	0	0.000	0	2.201
20.0	1.811	8	2.131	4	0.000	0	0.000	0	2.201
21.0	1.801	8	2.121	4	0.000	0	0.000	0	2.201
22.0	1.791	9	2.111	4	0.000	0	0.000	0	2.201
23.0	1.781	9	2.101	4	0.000	0	0.000	0	2.201
24.0	1.771	10	2.091	4	0.000	0	0.000	0	2.201
25.0	1.761	10	2.081	4	0.000	0	0.000	0	2.201
30.0	1.811	15	2.141	4	0.000	0	0.000	0	2.201
35.0	1.931	20	2.261	4	0.000	0	0.000	0	2.201
40.0	2.111	28	2.541	4	0.000	0	0.000	0	2.201
45.0	2.351	38	2.781	4	0.000	0	0.000	0	2.201
50.0	2.661	48	3.091	4	0.000	0	0.000	0	2.201

Figure 8. Calculated CO laser absorption coefficients for the mid-latitude summer model.

DATE	03/04/77	7	6	15
LASER LINE	1933.4053			
MODEL	MIDLATITUDE SUMMER			
NALFAE	3.000, FTAZ= 1.770			
ALT.	M20	CO2	CO	TOTAL
0.0	1.928E-0	1.850E-3	0.000E-0	1.928E-0
1.0	1.130E-0	1.509E-3	0.000E-0	1.130E-0
2.0	6.295E-1	1.236E-3	0.000E-0	6.295E-1
3.0	3.062E-1	1.011E-3	0.000E-0	3.062E-1
4.0	1.537E-1	8.261E-4	0.000E-0	1.537E-1
5.0	7.035E-2	6.722E-4	0.000E-0	7.035E-2
6.0	3.724E-2	5.437E-4	0.000E-0	3.724E-2
7.0	1.950E-2	4.360E-4	0.000E-0	1.950E-2
8.0	9.853E-3	3.815E-4	0.000E-0	9.853E-3
9.0	4.678E-3	2.801E-4	0.000E-0	4.678E-3
10.0	2.094E-3	2.035E-4	0.000E-0	2.094E-3
11.0	6.059E-4	1.761E-4	0.000E-0	6.059E-4
12.0	1.378E-4	1.487E-4	0.000E-0	1.378E-4
13.0	3.853E-5	1.075E-4	0.000E-0	3.853E-5
14.0	1.871E-5	7.853E-5	0.000E-0	1.871E-5
15.0	1.119E-5	5.670E-5	0.000E-0	1.119E-5
16.0	6.940E-6	4.134E-5	0.000E-0	6.940E-6
17.0	4.466E-6	3.029E-5	0.000E-0	4.466E-6
18.0	2.988E-6	2.213E-5	0.000E-0	2.988E-6
19.0	1.922E-6	1.686E-5	0.000E-0	1.922E-6
20.0	1.252E-6	1.267E-5	0.000E-0	1.252E-6
21.0	8.494E-7	9.494E-6	0.000E-0	8.494E-7
22.0	5.623E-7	6.800E-6	0.000E-0	5.623E-7
23.0	3.744E-7	4.893E-6	0.000E-0	3.744E-7
24.0	2.418E-7	3.266E-6	0.000E-0	2.418E-7
25.0	1.573E-7	2.296E-6	0.000E-0	1.573E-7
30.0	7.073E-8	1.090E-6	0.000E-0	7.073E-8
35.0	3.046E-8	4.314E-7	0.000E-0	3.046E-8
40.0	1.265E-8	1.636E-7	0.000E-0	1.265E-8
45.0	5.165E-9	6.790E-8	0.000E-0	5.165E-9
50.0	2.077E-9	2.611E-8	0.000E-0	2.077E-9

DATE	03/04/77	7	6	12
LASER LINE	1939.5252			
MODEL	MIDLATITUDE SUMMER			
NALFAE	3.000, FTAZ= 1.770			
ALT.	M20	CO2	CO	TOTAL
0.0	4.339E-0	4.084E-3	0.000E-0	4.339E-0
1.0	2.595E-0	4.102E-3	0.000E-0	2.595E-0
2.0	1.594E-0	4.159E-3	0.000E-0	1.594E-0
3.0	7.338E-1	4.197E-3	0.000E-0	7.338E-1
4.0	3.679E-1	4.159E-3	0.000E-0	3.679E-1
5.0	1.859E-1	4.174E-3	0.000E-0	1.859E-1
6.0	9.756E-2	4.146E-3	0.000E-0	9.756E-2
7.0	4.756E-2	4.110E-3	0.000E-0	4.756E-2
8.0	2.598E-2	4.075E-3	0.000E-0	2.598E-2
9.0	1.454E-2	3.905E-3	0.000E-0	1.454E-2
10.0	8.472E-3	3.508E-3	0.000E-0	8.472E-3
11.0	4.947E-3	3.088E-3	0.000E-0	4.947E-3
12.0	2.742E-3	2.742E-3	0.000E-0	2.742E-3
13.0	1.587E-3	2.472E-3	0.000E-0	1.587E-3
14.0	9.041E-4	2.247E-3	0.000E-0	9.041E-4
15.0	5.145E-4	2.065E-3	0.000E-0	5.145E-4
16.0	2.979E-4	1.878E-3	0.000E-0	2.979E-4
17.0	1.671E-4	1.692E-3	0.000E-0	1.671E-4
18.0	9.442E-5	1.516E-3	0.000E-0	9.442E-5
19.0	5.350E-5	1.350E-3	0.000E-0	5.350E-5
20.0	2.942E-5	1.188E-3	0.000E-0	2.942E-5
21.0	1.642E-5	1.041E-3	0.000E-0	1.642E-5
22.0	9.041E-6	9.041E-4	0.000E-0	9.041E-6
23.0	5.145E-6	7.853E-4	0.000E-0	5.145E-6
24.0	2.850E-6	6.800E-4	0.000E-0	2.850E-6
25.0	1.639E-6	5.849E-4	0.000E-0	1.639E-6
30.0	6.869E-7	4.893E-4	0.000E-0	6.869E-7
35.0	2.979E-7	4.090E-4	0.000E-0	2.979E-7
40.0	1.265E-7	3.346E-4	0.000E-0	1.265E-7
45.0	5.165E-8	2.611E-4	0.000E-0	5.165E-8
50.0	2.077E-8	1.922E-4	0.000E-0	2.077E-8

Figure 10. Calculated CO laser absorption coefficients for the mid-latitude summer model.

DATE	03/04/77	1966.8507	7	6	7
LASER LINE	MIDLATTITUDE SUMMER				
WAVELENGTH	WAVELENGTH	WAVELENGTH	WAVELENGTH	WAVELENGTH	WAVELENGTH
3.000	3.000	3.000	3.000	3.000	3.000
FTAZ	FTAZ	FTAZ	FTAZ	FTAZ	FTAZ
1.770	1.770	1.770	1.770	1.770	1.770
ALT.	0.0	0.0	0.0	0.0	0.0
1.0	8.703E-1	8.703E-1	8.703E-1	8.703E-1	8.703E-1
2.0	5.095E-1	5.095E-1	5.095E-1	5.095E-1	5.095E-1
3.0	2.826E-1	2.826E-1	2.826E-1	2.826E-1	2.826E-1
4.0	1.571E-1	1.571E-1	1.571E-1	1.571E-1	1.571E-1
5.0	8.635E-2	8.635E-2	8.635E-2	8.635E-2	8.635E-2
6.0	4.759E-2	4.759E-2	4.759E-2	4.759E-2	4.759E-2
7.0	2.616E-2	2.616E-2	2.616E-2	2.616E-2	2.616E-2
8.0	1.438E-2	1.438E-2	1.438E-2	1.438E-2	1.438E-2
9.0	8.205E-3	8.205E-3	8.205E-3	8.205E-3	8.205E-3
10.0	4.703E-3	4.703E-3	4.703E-3	4.703E-3	4.703E-3
11.0	2.712E-3	2.712E-3	2.712E-3	2.712E-3	2.712E-3
12.0	1.600E-3	1.600E-3	1.600E-3	1.600E-3	1.600E-3
13.0	9.545E-4	9.545E-4	9.545E-4	9.545E-4	9.545E-4
14.0	5.649E-4	5.649E-4	5.649E-4	5.649E-4	5.649E-4
15.0	3.355E-4	3.355E-4	3.355E-4	3.355E-4	3.355E-4
16.0	2.019E-4	2.019E-4	2.019E-4	2.019E-4	2.019E-4
17.0	1.215E-4	1.215E-4	1.215E-4	1.215E-4	1.215E-4
18.0	7.495E-5	7.495E-5	7.495E-5	7.495E-5	7.495E-5
19.0	4.618E-5	4.618E-5	4.618E-5	4.618E-5	4.618E-5
20.0	2.826E-5	2.826E-5	2.826E-5	2.826E-5	2.826E-5
21.0	1.695E-5	1.695E-5	1.695E-5	1.695E-5	1.695E-5
22.0	1.032E-5	1.032E-5	1.032E-5	1.032E-5	1.032E-5
23.0	6.392E-6	6.392E-6	6.392E-6	6.392E-6	6.392E-6
24.0	3.972E-6	3.972E-6	3.972E-6	3.972E-6	3.972E-6
25.0	2.492E-6	2.492E-6	2.492E-6	2.492E-6	2.492E-6
30.0	8.531E-7	8.531E-7	8.531E-7	8.531E-7	8.531E-7
35.0	2.692E-7	2.692E-7	2.692E-7	2.692E-7	2.692E-7
40.0	8.205E-8	8.205E-8	8.205E-8	8.205E-8	8.205E-8
45.0	2.616E-8	2.616E-8	2.616E-8	2.616E-8	2.616E-8
50.0	8.205E-9	8.205E-9	8.205E-9	8.205E-9	8.205E-9

DATE	03/04/77	1970.6642	7	6	4
LASER LINE	MIDLATTITUDE SUMMER				
WAVELENGTH	WAVELENGTH	WAVELENGTH	WAVELENGTH	WAVELENGTH	WAVELENGTH
3.000	3.000	3.000	3.000	3.000	3.000
FTAZ	FTAZ	FTAZ	FTAZ	FTAZ	FTAZ
1.770	1.770	1.770	1.770	1.770	1.770
ALT.	0.0	0.0	0.0	0.0	0.0
1.0	8.495E-1	8.495E-1	8.495E-1	8.495E-1	8.495E-1
2.0	4.659E-1	4.659E-1	4.659E-1	4.659E-1	4.659E-1
3.0	2.616E-1	2.616E-1	2.616E-1	2.616E-1	2.616E-1
4.0	1.438E-1	1.438E-1	1.438E-1	1.438E-1	1.438E-1
5.0	8.205E-2	8.205E-2	8.205E-2	8.205E-2	8.205E-2
6.0	4.703E-2	4.703E-2	4.703E-2	4.703E-2	4.703E-2
7.0	2.712E-2	2.712E-2	2.712E-2	2.712E-2	2.712E-2
8.0	1.600E-2	1.600E-2	1.600E-2	1.600E-2	1.600E-2
9.0	9.545E-3	9.545E-3	9.545E-3	9.545E-3	9.545E-3
10.0	5.649E-3	5.649E-3	5.649E-3	5.649E-3	5.649E-3
11.0	3.355E-3	3.355E-3	3.355E-3	3.355E-3	3.355E-3
12.0	2.019E-3	2.019E-3	2.019E-3	2.019E-3	2.019E-3
13.0	1.215E-3	1.215E-3	1.215E-3	1.215E-3	1.215E-3
14.0	7.495E-4	7.495E-4	7.495E-4	7.495E-4	7.495E-4
15.0	4.618E-4	4.618E-4	4.618E-4	4.618E-4	4.618E-4
16.0	2.826E-4	2.826E-4	2.826E-4	2.826E-4	2.826E-4
17.0	1.695E-4	1.695E-4	1.695E-4	1.695E-4	1.695E-4
18.0	1.032E-4	1.032E-4	1.032E-4	1.032E-4	1.032E-4
19.0	6.392E-5	6.392E-5	6.392E-5	6.392E-5	6.392E-5
20.0	3.972E-5	3.972E-5	3.972E-5	3.972E-5	3.972E-5
21.0	2.492E-5	2.492E-5	2.492E-5	2.492E-5	2.492E-5
22.0	1.571E-5	1.571E-5	1.571E-5	1.571E-5	1.571E-5
23.0	9.545E-6	9.545E-6	9.545E-6	9.545E-6	9.545E-6
24.0	5.649E-6	5.649E-6	5.649E-6	5.649E-6	5.649E-6
25.0	3.355E-6	3.355E-6	3.355E-6	3.355E-6	3.355E-6
30.0	1.215E-6	1.215E-6	1.215E-6	1.215E-6	1.215E-6
35.0	4.618E-7	4.618E-7	4.618E-7	4.618E-7	4.618E-7
40.0	1.600E-7	1.600E-7	1.600E-7	1.600E-7	1.600E-7
45.0	5.649E-8	5.649E-8	5.649E-8	5.649E-8	5.649E-8
50.0	1.954E-8	1.954E-8	1.954E-8	1.954E-8	1.954E-8

Figure 12. Calculated CO laser absorption coefficients for the mid-latitude summer model.

DATE	03/04/77	1974-4033	7 6 3	7 6 2
LASER LINE	1974-4033	1974-1079	1974-1079	1974-1079
MODEL	MIDLATHITUDE	MIDLATHITUDE	MIDLATHITUDE	MIDLATHITUDE
WAVELENGTH	3.000	3.000	3.000	3.000
ETA	1.770	1.770	1.770	1.770
ALT.	0.0	0.0	0.0	0.0
1.0	1.0	1.0	1.0	
2.0	2.0	2.0	2.0	
3.0	3.0	3.0	3.0	
4.0	4.0	4.0	4.0	
5.0	5.0	5.0	5.0	
6.0	6.0	6.0	6.0	
7.0	7.0	7.0	7.0	
8.0	8.0	8.0	8.0	
9.0	9.0	9.0	9.0	
10.0	10.0	10.0	10.0	
11.0	11.0	11.0	11.0	
12.0	12.0	12.0	12.0	
13.0	13.0	13.0	13.0	
14.0	14.0	14.0	14.0	
15.0	15.0	15.0	15.0	
16.0	16.0	16.0	16.0	
17.0	17.0	17.0	17.0	
18.0	18.0	18.0	18.0	
19.0	19.0	19.0	19.0	
20.0	20.0	20.0	20.0	
21.0	21.0	21.0	21.0	
22.0	22.0	22.0	22.0	
23.0	23.0	23.0	23.0	
24.0	24.0	24.0	24.0	
25.0	25.0	25.0	25.0	
26.0	26.0	26.0	26.0	
27.0	27.0	27.0	27.0	
28.0	28.0	28.0	28.0	
29.0	29.0	29.0	29.0	
30.0	30.0	30.0	30.0	
31.0	31.0	31.0	31.0	
32.0	32.0	32.0	32.0	
33.0	33.0	33.0	33.0	
34.0	34.0	34.0	34.0	
35.0	35.0	35.0	35.0	
36.0	36.0	36.0	36.0	
37.0	37.0	37.0	37.0	
38.0	38.0	38.0	38.0	
39.0	39.0	39.0	39.0	
40.0	40.0	40.0	40.0	
41.0	41.0	41.0	41.0	
42.0	42.0	42.0	42.0	
43.0	43.0	43.0	43.0	
44.0	44.0	44.0	44.0	
45.0	45.0	45.0	45.0	
46.0	46.0	46.0	46.0	
47.0	47.0	47.0	47.0	
48.0	48.0	48.0	48.0	
49.0	49.0	49.0	49.0	
50.0	50.0	50.0	50.0	

DATE	03/04/77	19A1-7778	7 6 1	7 6 2
LASER LINE	19A1-7778	19A1-7778	19A1-7778	19A1-7778
MODEL	MIDLATHITUDE	MIDLATHITUDE	MIDLATHITUDE	MIDLATHITUDE
WAVELENGTH	3.000	3.000	3.000	3.000
ETA	1.770	1.770	1.770	1.770
ALT.	0.0	0.0	0.0	0.0
1.0	1.0	1.0	1.0	
2.0	2.0	2.0	2.0	
3.0	3.0	3.0	3.0	
4.0	4.0	4.0	4.0	
5.0	5.0	5.0	5.0	
6.0	6.0	6.0	6.0	
7.0	7.0	7.0	7.0	
8.0	8.0	8.0	8.0	
9.0	9.0	9.0	9.0	
10.0	10.0	10.0	10.0	
11.0	11.0	11.0	11.0	
12.0	12.0	12.0	12.0	
13.0	13.0	13.0	13.0	
14.0	14.0	14.0	14.0	
15.0	15.0	15.0	15.0	
16.0	16.0	16.0	16.0	
17.0	17.0	17.0	17.0	
18.0	18.0	18.0	18.0	
19.0	19.0	19.0	19.0	
20.0	20.0	20.0	20.0	
21.0	21.0	21.0	21.0	
22.0	22.0	22.0	22.0	
23.0	23.0	23.0	23.0	
24.0	24.0	24.0	24.0	
25.0	25.0	25.0	25.0	
26.0	26.0	26.0	26.0	
27.0	27.0	27.0	27.0	
28.0	28.0	28.0	28.0	
29.0	29.0	29.0	29.0	
30.0	30.0	30.0	30.0	
31.0	31.0	31.0	31.0	
32.0	32.0	32.0	32.0	
33.0	33.0	33.0	33.0	
34.0	34.0	34.0	34.0	
35.0	35.0	35.0	35.0	
36.0	36.0	36.0	36.0	
37.0	37.0	37.0	37.0	
38.0	38.0	38.0	38.0	
39.0	39.0	39.0	39.0	
40.0	40.0	40.0	40.0	
41.0	41.0	41.0	41.0	
42.0	42.0	42.0	42.0	
43.0	43.0	43.0	43.0	
44.0	44.0	44.0	44.0	
45.0	45.0	45.0	45.0	
46.0	46.0	46.0	46.0	
47.0	47.0	47.0	47.0	
48.0	48.0	48.0	48.0	
49.0	49.0	49.0	49.0	
50.0	50.0	50.0	50.0	

Figure 13. Calculated CO laser absorption coefficients for the mid-latitude summer model.

DATE 03/04/77 1952-2043 6 5 15
LASER LINE MIDLATTITUDE SUMMER
MOPFLL: MIDLATTITUDE SUMMER
MALFA: 3.000, ETA: 1.770

ALT.	H2O	CO2	CO	TOTAL
0.0	1.485E-0	2.543E-4	0.000E-0	1.485E-0
1.0	7.820E-1	1.870E-4	0.000E-0	7.820E-1
2.0	5.444E-1	1.165E-4	0.000E-0	5.444E-1
3.0	4.019E-1	7.232E-5	0.000E-0	4.019E-1
4.0	3.081E-1	4.425E-5	0.000E-0	3.081E-1
5.0	2.468E-1	2.795E-5	0.000E-0	2.468E-1
6.0	1.998E-1	1.700E-5	0.000E-0	1.998E-1
7.0	1.620E-1	1.050E-5	0.000E-0	1.620E-1
8.0	1.300E-1	6.612E-6	0.000E-0	1.300E-1
9.0	1.020E-1	4.200E-6	0.000E-0	1.020E-1
10.0	7.900E-2	2.630E-6	0.000E-0	7.900E-2
11.0	6.150E-2	1.620E-6	0.000E-0	6.150E-2
12.0	4.850E-2	1.000E-6	0.000E-0	4.850E-2
13.0	3.800E-2	6.400E-7	0.000E-0	3.800E-2
14.0	2.900E-2	4.100E-7	0.000E-0	2.900E-2
15.0	2.200E-2	2.600E-7	0.000E-0	2.200E-2
16.0	1.650E-2	1.600E-7	0.000E-0	1.650E-2
17.0	1.250E-2	1.000E-7	0.000E-0	1.250E-2
18.0	9.500E-3	6.400E-8	0.000E-0	9.500E-3
19.0	7.200E-3	4.100E-8	0.000E-0	7.200E-3
20.0	5.500E-3	2.600E-8	0.000E-0	5.500E-3
21.0	4.200E-3	1.600E-8	0.000E-0	4.200E-3
22.0	3.200E-3	1.000E-8	0.000E-0	3.200E-3
23.0	2.400E-3	6.400E-9	0.000E-0	2.400E-3
24.0	1.800E-3	4.100E-9	0.000E-0	1.800E-3
25.0	1.350E-3	2.600E-9	0.000E-0	1.350E-3
30.0	7.500E-4	1.600E-9	0.000E-0	7.500E-4
35.0	4.500E-4	1.000E-9	0.000E-0	4.500E-4
40.0	2.700E-4	6.400E-10	0.000E-0	2.700E-4
45.0	1.600E-4	4.100E-10	0.000E-0	1.600E-4
50.0	9.500E-5	2.600E-10	0.000E-0	9.500E-5

DATE 03/04/77 1957-0480 6 5 14
LASER LINE MIDLATTITUDE SUMMER
MOPFLL: MIDLATTITUDE SUMMER
MALFA: 3.000, ETA: 1.770

ALT.	H2O	CO2	CO	TOTAL
0.0	4.157E-0	4.709E-3	0.000E-0	4.157E-0
1.0	2.783E-0	4.017E-3	0.000E-0	2.783E-0
2.0	1.780E-0	3.595E-3	0.000E-0	1.780E-0
3.0	1.000E-0	2.627E-3	0.000E-0	1.000E-0
4.0	5.850E-1	2.359E-3	0.000E-0	5.850E-1
5.0	3.130E-1	1.903E-3	0.000E-0	3.130E-1
6.0	1.946E-1	1.535E-3	0.000E-0	1.946E-1
7.0	1.208E-1	1.216E-3	0.000E-0	1.208E-1
8.0	6.926E-2	9.560E-4	0.000E-0	6.926E-2
9.0	4.045E-2	7.464E-4	0.000E-0	4.045E-2
10.0	2.170E-2	5.747E-4	0.000E-0	2.170E-2
11.0	1.166E-2	4.378E-4	0.000E-0	1.166E-2
12.0	6.291E-3	3.291E-4	0.000E-0	6.291E-3
13.0	3.443E-3	2.494E-4	0.000E-0	3.443E-3
14.0	1.892E-3	1.794E-4	0.000E-0	1.892E-3
15.0	1.000E-3	1.300E-4	0.000E-0	1.000E-3
16.0	5.450E-4	9.509E-5	0.000E-0	5.450E-4
17.0	2.853E-4	6.879E-5	0.000E-0	2.853E-4
18.0	1.465E-4	5.110E-5	0.000E-0	1.465E-4
19.0	7.453E-5	3.745E-5	0.000E-0	7.453E-5
20.0	4.161E-5	2.745E-5	0.000E-0	4.161E-5
21.0	2.277E-5	2.016E-5	0.000E-0	2.277E-5
22.0	1.266E-5	1.479E-5	0.000E-0	1.266E-5
23.0	6.925E-6	1.093E-5	0.000E-0	6.925E-6
24.0	3.752E-6	8.012E-6	0.000E-0	3.752E-6
25.0	2.024E-6	5.824E-6	0.000E-0	2.024E-6
30.0	1.057E-6	4.266E-6	0.000E-0	1.057E-6
35.0	6.095E-7	3.185E-6	0.000E-0	6.095E-7
40.0	3.525E-7	2.300E-6	0.000E-0	3.525E-7
45.0	2.000E-7	1.699E-6	0.000E-0	2.000E-7
50.0	1.199E-7	1.229E-6	0.000E-0	1.199E-7

DATE 03/04/77 1961-1603 6 5 13
LASER LINE MIDLATTITUDE SUMMER
MOPFLL: MIDLATTITUDE SUMMER
MALFA: 3.000, ETA: 1.770

ALT.	H2O	CO2	CO	TOTAL
0.0	6.543F-1	2.722E-4	0.000E-0	6.543E-1
1.0	2.779E-1	1.206E-4	0.000E-0	2.779E-1
2.0	1.700E-1	7.000E-5	0.000E-0	1.700E-1
3.0	1.033E-1	4.327E-5	0.000E-0	1.033E-1
4.0	6.748E-2	2.600E-5	0.000E-0	6.748E-2
5.0	4.379E-2	1.599E-5	0.000E-0	4.379E-2
6.0	2.842E-2	9.820E-6	0.000E-0	2.842E-2
7.0	1.847E-2	6.142E-6	0.000E-0	1.847E-2
8.0	1.200E-2	3.822E-6	0.000E-0	1.200E-2
9.0	7.851E-3	2.445E-6	0.000E-0	7.851E-3
10.0	5.150E-3	1.565E-6	0.000E-0	5.150E-3
11.0	3.400E-3	1.000E-6	0.000E-0	3.400E-3
12.0	2.250E-3	6.400E-7	0.000E-0	2.250E-3
13.0	1.492E-3	4.100E-7	0.000E-0	1.492E-3
14.0	9.870E-4	2.600E-7	0.000E-0	9.870E-4
15.0	6.500E-4	1.600E-7	0.000E-0	6.500E-4
16.0	4.250E-4	1.000E-7	0.000E-0	4.250E-4
17.0	2.800E-4	6.400E-8	0.000E-0	2.800E-4
18.0	1.800E-4	4.100E-8	0.000E-0	1.800E-4
19.0	1.200E-4	2.600E-8	0.000E-0	1.200E-4
20.0	8.000E-5	1.600E-8	0.000E-0	8.000E-5
21.0	5.300E-5	1.000E-8	0.000E-0	5.300E-5
22.0	3.500E-5	6.400E-9	0.000E-0	3.500E-5
23.0	2.300E-5	4.100E-9	0.000E-0	2.300E-5
24.0	1.500E-5	2.600E-9	0.000E-0	1.500E-5
25.0	1.000E-5	1.600E-9	0.000E-0	1.000E-5
30.0	6.000E-6	1.000E-9	0.000E-0	6.000E-6
35.0	3.600E-6	6.400E-10	0.000E-0	3.600E-6
40.0	2.160E-6	4.100E-10	0.000E-0	2.160E-6
45.0	1.296E-6	2.600E-10	0.000E-0	1.296E-6
50.0	7.776E-7	1.600E-10	0.000E-0	7.776E-7

DATE 03/04/77 1965-2388 6 5 12
LASER LINE MIDLATTITUDE SUMMER
MOPFLL: MIDLATTITUDE SUMMER
MALFA: 3.000, ETA: 1.770

ALT.	H2O	CO2	CO	TOTAL
0.0	5.320E-0	6.851E-3	0.000E-0	5.320E-0
1.0	3.412E-0	7.985E-3	0.000E-0	3.412E-0
2.0	2.200E-0	6.960E-3	0.000E-0	2.200E-0
3.0	1.350E-0	5.975E-3	0.000E-0	1.350E-0
4.0	8.150E-1	5.055E-3	0.000E-0	8.150E-1
5.0	4.650E-1	4.200E-3	0.000E-0	4.650E-1
6.0	2.850E-1	3.426E-3	0.000E-0	2.850E-1
7.0	1.750E-1	2.757E-3	0.000E-0	1.750E-1
8.0	1.050E-1	2.199E-3	0.000E-0	1.050E-1
9.0	6.250E-2	1.652E-3	0.000E-0	6.250E-2
10.0	3.850E-2	1.244E-3	0.000E-0	3.850E-2
11.0	2.400E-2	9.271E-4	0.000E-0	2.400E-2
12.0	1.550E-2	6.770E-4	0.000E-0	1.550E-2
13.0	1.000E-2	5.050E-4	0.000E-0	1.000E-2
14.0	6.500E-3	3.750E-4	0.000E-0	6.500E-3
15.0	4.200E-3	2.800E-4	0.000E-0	4.200E-3
16.0	2.800E-3	2.050E-4	0.000E-0	2.800E-3
17.0	1.800E-3	1.500E-4	0.000E-0	1.800E-3
18.0	1.200E-3	1.050E-4	0.000E-0	1.200E-3
19.0	8.000E-4	7.700E-5	0.000E-0	8.000E-4
20.0	5.300E-4	5.700E-5	0.000E-0	5.300E-4
21.0	3.500E-4	4.200E-5	0.000E-0	3.500E-4
22.0	2.300E-4	3.100E-5	0.000E-0	2.300E-4
23.0	1.500E-4	2.300E-5	0.000E-0	1.500E-4
24.0	1.000E-4	1.700E-5	0.000E-0	1.000E-4
25.0	6.500E-5	1.250E-5	0.000E-0	6.500E-5
30.0	4.000E-5	7.700E-6	0.000E-0	4.000E-5
35.0	2.500E-5	5.100E-6	0.000E-0	2.500E-5
40.0	1.600E-5	3.400E-6	0.000E-0	1.600E-5
45.0	1.000E-5	2.300E-6	0.000E-0	1.000E-5
50.0	6.500E-6	1.550E-6	0.000E-0	6.500E-6

Figure 14. Calculated CO laser absorption coefficients for the mid-latitude summer model.

DATE 03/04/77									
LASER LINE 1669-2880									
MODEL: MID-LATITUDE SUMMER									
NALFA= 3.000, ETA= 1.770									
ALT.	H2O	CO2	CO	CO3	0	0	0	0	TOTAL
0.0	4.092E-0	9.599E-5	0.000E-0	0.000E-0	1.432E-9	4.092E-0	0.000E-0	0.000E-0	4.092E-0
1.0	4.590E-0	7.492E-5	0.000E-0	0.000E-0	1.432E-9	2.390E-0	0.000E-0	0.000E-0	2.390E-0
2.0	1.519E-0	5.740E-5	0.000E-0	0.000E-0	1.432E-9	1.319E-0	0.000E-0	0.000E-0	1.319E-0
3.0	6.317E-1	4.288E-5	0.000E-0	0.000E-0	1.432E-9	6.317E-1	0.000E-0	0.000E-0	6.317E-1
4.0	3.115E-1	3.181E-5	0.000E-0	0.000E-0	1.432E-9	3.115E-1	0.000E-0	0.000E-0	3.115E-1
5.0	1.599E-1	2.356E-5	0.000E-0	0.000E-0	1.432E-9	1.599E-1	0.000E-0	0.000E-0	1.599E-1
6.0	7.261E-2	1.696E-5	0.000E-0	0.000E-0	1.432E-9	7.261E-2	0.000E-0	0.000E-0	7.261E-2
7.0	3.724E-2	1.215E-5	0.000E-0	0.000E-0	1.432E-9	3.724E-2	0.000E-0	0.000E-0	3.724E-2
8.0	1.760E-2	8.530E-6	0.000E-0	0.000E-0	1.432E-9	1.760E-2	0.000E-0	0.000E-0	1.760E-2
9.0	8.244E-3	4.144E-6	0.000E-0	0.000E-0	1.432E-9	8.244E-3	0.000E-0	0.000E-0	8.244E-3
10.0	3.949E-3	2.667E-6	0.000E-0	0.000E-0	1.432E-9	3.949E-3	0.000E-0	0.000E-0	3.949E-3
11.0	1.050E-3	1.931E-6	0.000E-0	0.000E-0	1.432E-9	1.050E-3	0.000E-0	0.000E-0	1.050E-3
12.0	5.855E-4	1.303E-6	0.000E-0	0.000E-0	1.432E-9	5.855E-4	0.000E-0	0.000E-0	5.855E-4
13.0	2.778E-4	9.248E-7	0.000E-0	0.000E-0	1.432E-9	2.778E-4	0.000E-0	0.000E-0	2.778E-4
14.0	1.861E-4	6.682E-7	0.000E-0	0.000E-0	1.432E-9	1.861E-4	0.000E-0	0.000E-0	1.861E-4
15.0	1.075E-4	5.020E-7	0.000E-0	0.000E-0	1.432E-9	1.075E-4	0.000E-0	0.000E-0	1.075E-4
16.0	5.917E-5	3.678E-7	0.000E-0	0.000E-0	1.432E-9	5.917E-5	0.000E-0	0.000E-0	5.917E-5
17.0	3.268E-5	2.688E-7	0.000E-0	0.000E-0	1.432E-9	3.268E-5	0.000E-0	0.000E-0	3.268E-5
18.0	1.801E-5	1.998E-7	0.000E-0	0.000E-0	1.432E-9	1.801E-5	0.000E-0	0.000E-0	1.801E-5
19.0	7.494E-6	1.485E-7	0.000E-0	0.000E-0	1.432E-9	7.494E-6	0.000E-0	0.000E-0	7.494E-6
20.0	3.191E-6	1.107E-7	0.000E-0	0.000E-0	1.432E-9	3.191E-6	0.000E-0	0.000E-0	3.191E-6
21.0	1.645E-6	8.243E-8	0.000E-0	0.000E-0	1.432E-9	1.645E-6	0.000E-0	0.000E-0	1.645E-6
22.0	8.095E-7	6.277E-8	0.000E-0	0.000E-0	1.432E-9	8.095E-7	0.000E-0	0.000E-0	8.095E-7
23.0	4.543E-7	4.660E-8	0.000E-0	0.000E-0	1.432E-9	4.543E-7	0.000E-0	0.000E-0	4.543E-7
24.0	2.544E-7	3.509E-8	0.000E-0	0.000E-0	1.432E-9	2.544E-7	0.000E-0	0.000E-0	2.544E-7
25.0	1.305E-7	2.125E-8	0.000E-0	0.000E-0	1.432E-9	1.305E-7	0.000E-0	0.000E-0	1.305E-7
30.0	3.819E-7	2.483E-9	0.000E-0	0.000E-0	1.432E-9	3.819E-7	0.000E-0	0.000E-0	3.819E-7
35.0	1.010E-7	8.055E-10	0.000E-0	0.000E-0	1.432E-9	1.010E-7	0.000E-0	0.000E-0	1.010E-7
40.0	3.027E-8	2.646E-10	0.000E-0	0.000E-0	1.432E-9	3.027E-8	0.000E-0	0.000E-0	3.027E-8
45.0	6.350E-9	8.395E-11	0.000E-0	0.000E-0	1.432E-9	6.350E-9	0.000E-0	0.000E-0	6.350E-9
50.0	0.000E-0	0.000E-0	0.000E-0	0.000E-0	1.432E-9	0.000E-0	0.000E-0	0.000E-0	0.000E-0

DATE 03/04/77									
LASER LINE 1981-2189									
MODEL: MID-LATITUDE SUMMER									
NALFA= 3.000, ETA= 1.770									
ALT.	H2O	CO2	CO	CO3	0	0	0	0	TOTAL
0.0	5.326E-1	6.813E-5	0.000E-0	0.000E-0	1.077E-7	5.326E-1	0.000E-0	0.000E-0	5.326E-1
1.0	3.568E-1	6.717E-5	0.000E-0	0.000E-0	1.077E-7	3.568E-1	0.000E-0	0.000E-0	3.568E-1
2.0	1.777E-1	5.036E-5	0.000E-0	0.000E-0	1.077E-7	1.777E-1	0.000E-0	0.000E-0	1.777E-1
3.0	8.720E-2	3.691E-5	0.000E-0	0.000E-0	1.077E-7	8.720E-2	0.000E-0	0.000E-0	8.720E-2
4.0	4.417E-2	2.647E-5	0.000E-0	0.000E-0	1.077E-7	4.417E-2	0.000E-0	0.000E-0	4.417E-2
5.0	2.063E-2	1.937E-5	0.000E-0	0.000E-0	1.077E-7	2.063E-2	0.000E-0	0.000E-0	2.063E-2
6.0	1.033E-2	1.380E-5	0.000E-0	0.000E-0	1.077E-7	1.033E-2	0.000E-0	0.000E-0	1.033E-2
7.0	5.783E-3	9.685E-6	0.000E-0	0.000E-0	1.077E-7	5.783E-3	0.000E-0	0.000E-0	5.783E-3
8.0	2.851E-3	6.650E-6	0.000E-0	0.000E-0	1.077E-7	2.851E-3	0.000E-0	0.000E-0	2.851E-3
9.0	1.416E-3	4.556E-6	0.000E-0	0.000E-0	1.077E-7	1.416E-3	0.000E-0	0.000E-0	1.416E-3
10.0	6.495E-4	3.029E-6	0.000E-0	0.000E-0	1.077E-7	6.495E-4	0.000E-0	0.000E-0	6.495E-4
11.0	3.248E-4	2.022E-6	0.000E-0	0.000E-0	1.077E-7	3.248E-4	0.000E-0	0.000E-0	3.248E-4
12.0	1.648E-4	1.398E-6	0.000E-0	0.000E-0	1.077E-7	1.648E-4	0.000E-0	0.000E-0	1.648E-4
13.0	8.244E-5	9.862E-7	0.000E-0	0.000E-0	1.077E-7	8.244E-5	0.000E-0	0.000E-0	8.244E-5
14.0	4.144E-5	6.109E-7	0.000E-0	0.000E-0	1.077E-7	4.144E-5	0.000E-0	0.000E-0	4.144E-5
15.0	2.144E-5	4.310E-7	0.000E-0	0.000E-0	1.077E-7	2.144E-5	0.000E-0	0.000E-0	2.144E-5
16.0	1.144E-5	3.015E-7	0.000E-0	0.000E-0	1.077E-7	1.144E-5	0.000E-0	0.000E-0	1.144E-5
17.0	6.144E-6	2.157E-7	0.000E-0	0.000E-0	1.077E-7	6.144E-6	0.000E-0	0.000E-0	6.144E-6
18.0	3.144E-6	1.522E-7	0.000E-0	0.000E-0	1.077E-7	3.144E-6	0.000E-0	0.000E-0	3.144E-6
19.0	1.513E-6	1.090E-7	0.000E-0	0.000E-0	1.077E-7	1.513E-6	0.000E-0	0.000E-0	1.513E-6
20.0	7.241E-7	6.665E-8	0.000E-0	0.000E-0	1.077E-7	7.241E-7	0.000E-0	0.000E-0	7.241E-7
21.0	3.257E-7	4.806E-8	0.000E-0	0.000E-0	1.077E-7	3.257E-7	0.000E-0	0.000E-0	3.257E-7
22.0	1.257E-7	3.458E-8	0.000E-0	0.000E-0	1.077E-7	1.257E-7	0.000E-0	0.000E-0	1.257E-7
23.0	5.465E-8	2.486E-8	0.000E-0	0.000E-0	1.077E-7	5.465E-8	0.000E-0	0.000E-0	5.465E-8
24.0	2.073E-8	1.760E-8	0.000E-0	0.000E-0	1.077E-7	2.073E-8	0.000E-0	0.000E-0	2.073E-8
25.0	1.066E-8	1.260E-8	0.000E-0	0.000E-0	1.077E-7	1.066E-8	0.000E-0	0.000E-0	1.066E-8
30.0	3.443E-8	6.669E-9	0.000E-0	0.000E-0	1.077E-7	3.443E-8	0.000E-0	0.000E-0	3.443E-8
35.0	6.511E-8	1.943E-9	0.000E-0	0.000E-0	1.077E-7	6.511E-8	0.000E-0	0.000E-0	6.511E-8
40.0	1.625E-8	6.203E-10	0.000E-0	0.000E-0	1.077E-7	1.625E-8	0.000E-0	0.000E-0	1.625E-8
45.0	4.660E-9	2.049E-10	0.000E-0	0.000E-0	1.077E-7	4.660E-9	0.000E-0	0.000E-0	4.660E-9
50.0	9.865E-10	6.831E-11	0.000E-0	0.000E-0	1.077E-7	9.865E-10	0.000E-0	0.000E-0	9.865E-10

Figure 15. Calculated CO laser absorption coefficients for the mid-latitude summer model.

DATE	03/04/77	5	4	15
LASER LINE	1982.7649	MIDLATITUDE SUMMER		
MODEL	3.000	ETA=	1.770	0.000
MALFA=	3.000	ETA=	1.770	0.000
ALT.	0.0	0.0	0.0	0.0
1.0	0.000	0.000	0.000	0.000
2.0	0.000	0.000	0.000	0.000
3.0	0.000	0.000	0.000	0.000
4.0	0.000	0.000	0.000	0.000
5.0	0.000	0.000	0.000	0.000
6.0	0.000	0.000	0.000	0.000
7.0	0.000	0.000	0.000	0.000
8.0	0.000	0.000	0.000	0.000
9.0	0.000	0.000	0.000	0.000
10.0	0.000	0.000	0.000	0.000
11.0	0.000	0.000	0.000	0.000
12.0	0.000	0.000	0.000	0.000
13.0	0.000	0.000	0.000	0.000
14.0	0.000	0.000	0.000	0.000
15.0	0.000	0.000	0.000	0.000
16.0	0.000	0.000	0.000	0.000
17.0	0.000	0.000	0.000	0.000
18.0	0.000	0.000	0.000	0.000
19.0	0.000	0.000	0.000	0.000
20.0	0.000	0.000	0.000	0.000
21.0	0.000	0.000	0.000	0.000
22.0	0.000	0.000	0.000	0.000
23.0	0.000	0.000	0.000	0.000
24.0	0.000	0.000	0.000	0.000
25.0	0.000	0.000	0.000	0.000
30.0	0.000	0.000	0.000	0.000
35.0	0.000	0.000	0.000	0.000
40.0	0.000	0.000	0.000	0.000
45.0	0.000	0.000	0.000	0.000
50.0	0.000	0.000	0.000	0.000

DATE	03/04/77	5	4	15
LASER LINE	1982.7649	MIDLATITUDE SUMMER		
MODEL	3.000	ETA=	1.770	0.000
MALFA=	3.000	ETA=	1.770	0.000
ALT.	0.0	0.0	0.0	0.0
1.0	0.000	0.000	0.000	0.000
2.0	0.000	0.000	0.000	0.000
3.0	0.000	0.000	0.000	0.000
4.0	0.000	0.000	0.000	0.000
5.0	0.000	0.000	0.000	0.000
6.0	0.000	0.000	0.000	0.000
7.0	0.000	0.000	0.000	0.000
8.0	0.000	0.000	0.000	0.000
9.0	0.000	0.000	0.000	0.000
10.0	0.000	0.000	0.000	0.000
11.0	0.000	0.000	0.000	0.000
12.0	0.000	0.000	0.000	0.000
13.0	0.000	0.000	0.000	0.000
14.0	0.000	0.000	0.000	0.000
15.0	0.000	0.000	0.000	0.000
16.0	0.000	0.000	0.000	0.000
17.0	0.000	0.000	0.000	0.000
18.0	0.000	0.000	0.000	0.000
19.0	0.000	0.000	0.000	0.000
20.0	0.000	0.000	0.000	0.000
21.0	0.000	0.000	0.000	0.000
22.0	0.000	0.000	0.000	0.000
23.0	0.000	0.000	0.000	0.000
24.0	0.000	0.000	0.000	0.000
25.0	0.000	0.000	0.000	0.000
30.0	0.000	0.000	0.000	0.000
35.0	0.000	0.000	0.000	0.000
40.0	0.000	0.000	0.000	0.000
45.0	0.000	0.000	0.000	0.000
50.0	0.000	0.000	0.000	0.000

Figure 18. Calculated CO laser absorption coefficients for the mid-latitude summer model.

DATE 03/04/77
 LASER LINE 2030.3080
 MODEL: MID-LATITUDE SUMMER
 WAVELENGTH 3.000, EIA= 1.770

ALT.	H2O	CO2	n3	CO	0	TOTAL
0.0	3.524E-1	4.266E-4	7.629E-9	9.929E-6	3.328E-1	
1.0	1.950E-1	3.272E-4	6.429E-9	7.715E-6	1.953E-1	
2.0	1.079E-1	2.479E-4	5.364E-9	5.942E-6	1.076E-1	
3.0	5.107E-2	1.849E-4	4.510E-9	4.510E-6	5.107E-2	
4.0	2.498E-2	1.371E-4	3.776E-9	3.415E-6	2.510E-2	
5.0	1.170E-2	1.014E-4	3.171E-9	2.569E-6	1.170E-2	
6.0	5.899E-3	7.461E-5	2.617E-9	1.918E-6	5.761E-3	
7.0	2.879E-3	5.445E-5	2.224E-9	1.416E-6	2.924E-3	
8.0	1.358E-3	3.842E-5	1.817E-9	1.045E-6	1.377E-3	
9.0	6.300E-4	2.872E-5	1.528E-9	7.560E-7	6.601E-4	
10.0	2.724E-4	2.070E-5	1.270E-9	5.434E-7	2.936E-4	
11.0	1.180E-4	1.480E-5	1.070E-9	3.903E-7	9.194E-5	
12.0	5.289E-5	1.060E-5	8.918E-10	2.749E-7	2.776E-5	
13.0	2.369E-5	7.769E-6	7.498E-10	1.930E-7	1.930E-5	
14.0	1.000E-5	5.691E-6	6.348E-10	1.410E-7	7.734E-6	
15.0	4.199E-6	4.097E-6	5.409E-10	1.018E-7	5.475E-6	
16.0	1.743E-6	2.997E-6	4.589E-10	7.443E-8	4.002E-6	
17.0	7.143E-7	2.105E-6	3.943E-10	5.433E-8	2.966E-6	
18.0	2.849E-7	1.495E-6	3.348E-10	3.939E-8	2.051E-6	
19.0	1.179E-7	1.079E-6	2.898E-10	2.739E-8	1.508E-6	
20.0	4.019E-7	8.162E-7	2.502E-10	1.608E-8	1.250E-6	
21.0	1.462E-7	6.382E-7	2.164E-10	1.105E-8	9.451E-7	
22.0	5.265E-7	4.701E-7	1.874E-10	7.505E-9	6.451E-7	
23.0	1.890E-7	3.490E-7	1.629E-10	5.356E-9	4.681E-7	
24.0	6.899E-7	2.579E-7	1.416E-10	3.768E-9	3.450E-7	
25.0	2.459E-7	1.916E-7	1.215E-10	2.699E-9	2.459E-7	
30.0	1.156E-7	9.500E-8	6.110E-11	1.192E-9	1.156E-7	
35.0	5.454E-8	4.842E-8	3.141E-11	5.115E-10	5.454E-8	
40.0	2.429E-8	2.219E-8	1.634E-11	2.429E-10	2.429E-8	
45.0	1.045E-8	1.045E-8	8.151E-12	1.045E-10	1.045E-8	
50.0	4.450E-9	3.261E-10	5.045E-13	7.971E-13	4.450E-9	

DATE 03/04/77
 LASER LINE 2030.3080
 MODEL: MID-LATITUDE SUMMER
 WAVELENGTH 3.000, EIA= 1.770

ALT.	H2O	CO2	n3	CO	0	TOTAL
0.0	3.524E-1	4.266E-4	7.629E-9	9.929E-6	3.328E-1	
1.0	1.950E-1	3.272E-4	6.429E-9	7.715E-6	1.953E-1	
2.0	1.079E-1	2.479E-4	5.364E-9	5.942E-6	1.076E-1	
3.0	5.107E-2	1.849E-4	4.510E-9	4.510E-6	5.107E-2	
4.0	2.498E-2	1.371E-4	3.776E-9	3.415E-6	2.510E-2	
5.0	1.170E-2	1.014E-4	3.171E-9	2.569E-6	1.170E-2	
6.0	5.899E-3	7.461E-5	2.617E-9	1.918E-6	5.761E-3	
7.0	2.879E-3	5.445E-5	2.224E-9	1.416E-6	2.924E-3	
8.0	1.358E-3	3.842E-5	1.817E-9	1.045E-6	1.377E-3	
9.0	6.300E-4	2.872E-5	1.528E-9	7.560E-7	6.601E-4	
10.0	2.724E-4	2.070E-5	1.270E-9	5.434E-7	2.936E-4	
11.0	1.180E-4	1.480E-5	1.070E-9	3.903E-7	9.194E-5	
12.0	5.289E-5	1.060E-5	8.918E-10	2.749E-7	2.776E-5	
13.0	2.369E-5	7.769E-6	7.498E-10	1.930E-7	1.930E-5	
14.0	1.000E-5	5.691E-6	6.348E-10	1.410E-7	7.734E-6	
15.0	4.199E-6	4.097E-6	5.409E-10	1.018E-7	5.475E-6	
16.0	1.743E-6	2.997E-6	4.589E-10	7.443E-8	4.002E-6	
17.0	7.143E-7	2.105E-6	3.943E-10	5.433E-8	2.966E-6	
18.0	2.849E-7	1.495E-6	3.348E-10	3.939E-8	2.051E-6	
19.0	1.179E-7	1.079E-6	2.898E-10	2.739E-8	1.508E-6	
20.0	4.019E-7	8.162E-7	2.502E-10	1.608E-8	1.250E-6	
21.0	1.462E-7	6.382E-7	2.164E-10	1.105E-8	9.451E-7	
22.0	5.265E-7	4.701E-7	1.874E-10	7.505E-9	6.451E-7	
23.0	1.890E-7	3.490E-7	1.629E-10	5.356E-9	4.681E-7	
24.0	6.899E-7	2.579E-7	1.416E-10	3.768E-9	3.450E-7	
25.0	2.459E-7	1.916E-7	1.215E-10	2.699E-9	2.459E-7	
30.0	1.156E-7	9.500E-8	6.110E-11	1.192E-9	1.156E-7	
35.0	5.454E-8	4.842E-8	3.141E-11	5.115E-10	5.454E-8	
40.0	2.429E-8	2.219E-8	1.634E-11	2.429E-10	2.429E-8	
45.0	1.045E-8	1.045E-8	8.151E-12	1.045E-10	1.045E-8	
50.0	4.450E-9	3.261E-10	5.045E-13	7.971E-13	4.450E-9	

Figure 21. Calculated CO laser absorption coefficients for the mid-latitude summer model.

DATE 03/04/77 2008.5519 4 3 14
 LASER LINE 2008.5519
 MODEL: MIDLATITUDE SUMMER
 NALFAZ 3.000, FIAZ 1.770

ALT.	H2O	CO2	O3	CO	TOTAL
0.0	4.220E-1	2.53E-4	0.000E-0	2.315E-5	4.243E-1
1.0	2.455E-1	1.107E-4	0.000E-0	1.955E-5	2.445E-1
2.0	1.358E-1	1.331E-4	0.000E-0	1.631E-5	1.337E-1
3.0	8.278E-2	1.319E-4	0.000E-0	1.298E-5	8.296E-2
4.0	5.068E-2	1.319E-4	0.000E-0	1.023E-5	5.079E-2
5.0	3.068E-2	1.319E-4	0.000E-0	7.962E-6	3.078E-2
6.0	1.868E-2	1.319E-4	0.000E-0	6.055E-6	1.877E-2
7.0	1.068E-2	1.319E-4	0.000E-0	4.585E-6	1.086E-2
8.0	5.908E-3	1.319E-4	0.000E-0	3.320E-6	5.927E-3
9.0	3.148E-3	1.319E-4	0.000E-0	2.408E-6	3.174E-3
10.0	1.748E-3	1.319E-4	0.000E-0	1.691E-6	1.763E-3
11.0	9.488E-4	1.319E-4	0.000E-0	1.188E-6	9.506E-4
12.0	5.108E-4	1.319E-4	0.000E-0	7.992E-7	5.158E-4
13.0	2.728E-4	1.319E-4	0.000E-0	5.375E-7	2.780E-4
14.0	1.428E-4	1.319E-4	0.000E-0	3.697E-7	1.438E-4
15.0	7.688E-5	1.319E-4	0.000E-0	2.498E-7	7.745E-5
16.0	4.188E-5	1.319E-4	0.000E-0	1.622E-7	4.205E-5
17.0	2.288E-5	1.319E-4	0.000E-0	1.056E-7	2.348E-5
18.0	1.248E-5	1.319E-4	0.000E-0	6.938E-8	1.268E-5
19.0	6.688E-6	1.319E-4	0.000E-0	4.538E-8	6.738E-6
20.0	3.688E-6	1.319E-4	0.000E-0	3.038E-8	3.738E-6
21.0	2.088E-6	1.319E-4	0.000E-0	2.038E-8	2.088E-6
22.0	1.188E-6	1.319E-4	0.000E-0	1.338E-8	1.188E-6
23.0	6.488E-7	1.319E-4	0.000E-0	8.938E-9	6.488E-7
24.0	3.588E-7	1.319E-4	0.000E-0	5.938E-9	3.588E-7
25.0	1.988E-7	1.319E-4	0.000E-0	3.938E-9	1.988E-7
26.0	1.088E-7	1.319E-4	0.000E-0	2.638E-9	1.088E-7
27.0	5.888E-8	1.319E-4	0.000E-0	1.738E-9	5.888E-8
28.0	3.188E-8	1.319E-4	0.000E-0	1.138E-9	3.188E-8
29.0	1.688E-8	1.319E-4	0.000E-0	7.38E-10	1.688E-8
30.0	8.888E-9	1.319E-4	0.000E-0	4.88E-10	8.888E-9
40.0	3.088E-9	1.319E-4	0.000E-0	1.68E-10	3.088E-9
45.0	1.688E-9	1.319E-4	0.000E-0	9.38E-11	1.688E-9
50.0	8.888E-10	1.319E-4	0.000E-0	5.18E-11	8.888E-10

DATE 03/04/77 2016.8421 4 3 12
 LASER LINE 2016.8421
 MODEL: MIDLATITUDE SUMMER
 NALFAZ 3.000, FIAZ 1.770

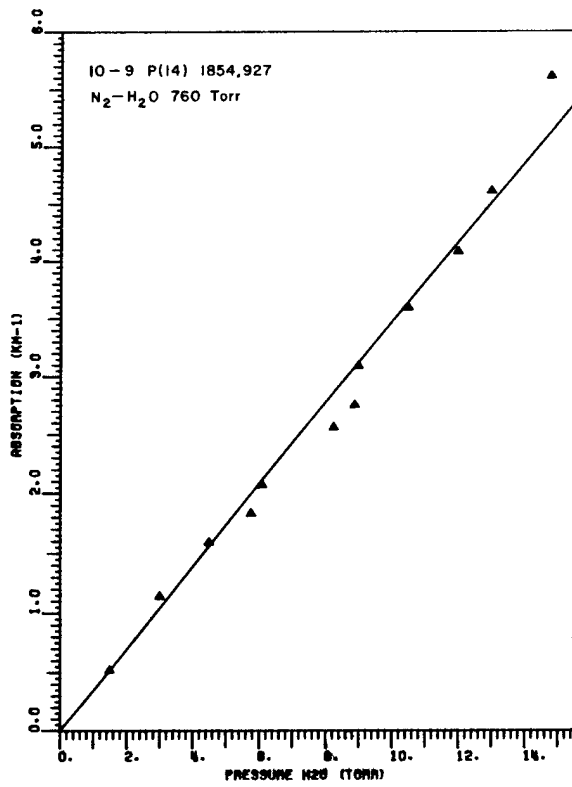
ALT.	H2O	CO2	O3	CO	TOTAL
0.0	6.970E-1	7.599E-5	0.000E-0	6.887E-6	6.971E-1
1.0	4.191E-1	4.062E-5	0.000E-0	5.201E-6	4.192E-1
2.0	2.591E-1	4.262E-5	0.000E-0	3.862E-6	2.591E-1
3.0	1.691E-1	3.811E-5	0.000E-0	2.801E-6	1.691E-1
4.0	9.091E-2	3.004E-5	0.000E-0	2.023E-6	9.091E-2
5.0	5.091E-2	2.354E-5	0.000E-0	1.451E-6	5.091E-2
6.0	2.891E-2	1.831E-5	0.000E-0	1.031E-6	2.891E-2
7.0	1.691E-2	1.401E-5	0.000E-0	7.232E-7	1.691E-2
8.0	9.191E-3	1.081E-5	0.000E-0	5.154E-7	9.191E-3
9.0	5.191E-3	8.217E-6	0.000E-0	3.637E-7	5.191E-3
10.0	2.891E-3	6.299E-6	0.000E-0	2.517E-7	2.891E-3
11.0	1.691E-3	4.699E-6	0.000E-0	1.757E-7	1.691E-3
12.0	9.191E-4	3.499E-6	0.000E-0	1.257E-7	9.191E-4
13.0	5.191E-4	2.599E-6	0.000E-0	8.57E-8	5.191E-4
14.0	2.891E-4	1.899E-6	0.000E-0	5.955E-8	2.891E-4
15.0	1.691E-4	1.399E-6	0.000E-0	4.255E-8	1.691E-4
16.0	9.191E-5	9.725E-7	0.000E-0	3.055E-8	9.191E-5
17.0	5.191E-5	7.122E-7	0.000E-0	2.195E-8	5.191E-5
18.0	2.891E-5	5.203E-7	0.000E-0	1.595E-8	2.891E-5
19.0	1.691E-5	3.813E-7	0.000E-0	1.125E-8	1.691E-5
20.0	9.191E-6	2.813E-7	0.000E-0	7.95E-9	9.191E-6
21.0	5.191E-6	2.098E-7	0.000E-0	5.65E-9	5.191E-6
22.0	2.891E-6	1.517E-7	0.000E-0	4.05E-9	2.891E-6
23.0	1.691E-6	1.117E-7	0.000E-0	2.85E-9	1.691E-6
24.0	9.191E-7	8.199E-8	0.000E-0	2.05E-9	9.191E-7
25.0	5.191E-7	6.060E-8	0.000E-0	1.45E-9	5.191E-7
26.0	2.891E-7	4.455E-8	0.000E-0	1.05E-9	2.891E-7
27.0	1.691E-7	3.250E-8	0.000E-0	7.5E-10	1.691E-7
28.0	9.191E-8	2.350E-8	0.000E-0	5.3E-10	9.191E-8
29.0	5.191E-8	1.750E-8	0.000E-0	3.8E-10	5.191E-8
30.0	2.891E-8	1.250E-8	0.000E-0	2.7E-10	2.891E-8
40.0	1.691E-8	7.500E-9	0.000E-0	1.5E-10	1.691E-8
45.0	9.191E-9	5.000E-9	0.000E-0	8.5E-11	9.191E-9
50.0	5.191E-9	3.500E-9	0.000E-0	5.0E-11	5.191E-9

Figure 22. Calculated CO laser absorption coefficients for the mid-latitude summer model.

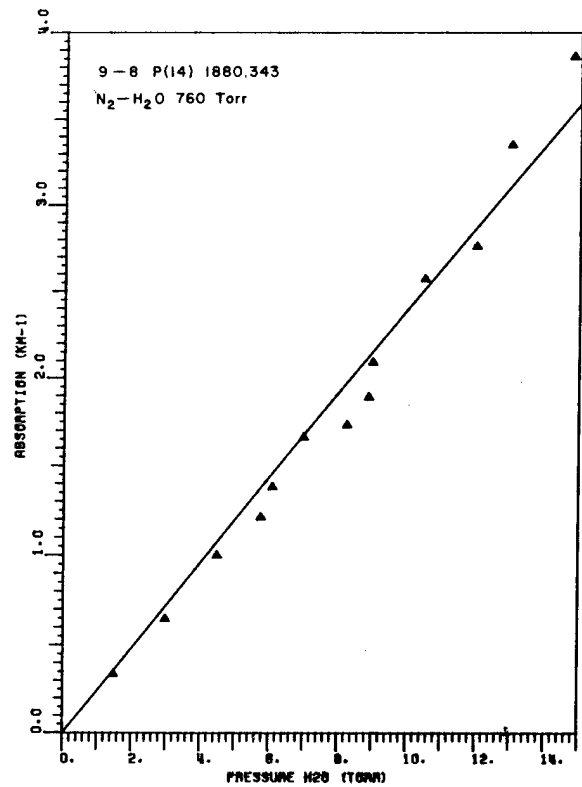
DATE 03/04/77											
LASER LINE 2030.4082											
MODEL: MIDLATTITUDE SUMMER											
NALFAZ 3.000, ETA= 1.770											
3 2 14											
H2O 0											
CO 0											
ALT. 0.0											
TOTAL 7.766E-1											
1.0 7.766E-1											
2.0 4.487E-1											
3.0 2.431E-1											
4.0 1.355E-1											
5.0 7.452E-2											
6.0 4.045E-2											
7.0 2.387E-2											
8.0 1.406E-2											
9.0 8.051E-3											
10.0 4.625E-3											
11.0 2.595E-3											
12.0 1.453E-3											
13.0 8.087E-4											
14.0 4.502E-4											
15.0 2.537E-4											
16.0 1.407E-4											
17.0 7.826E-5											
18.0 4.364E-5											
19.0 2.431E-5											
20.0 1.355E-5											
21.0 7.452E-6											
22.0 4.045E-6											
23.0 2.387E-6											
24.0 1.406E-6											
25.0 8.051E-7											
26.0 4.625E-7											
27.0 2.595E-7											
28.0 1.453E-7											
29.0 8.087E-8											
30.0 4.502E-8											
31.0 2.537E-8											
32.0 1.407E-8											
33.0 7.826E-9											
34.0 4.364E-9											
35.0 2.431E-9											
36.0 1.355E-9											
37.0 7.452E-10											
38.0 4.045E-10											
39.0 2.387E-10											
40.0 1.406E-10											
41.0 8.051E-11											
42.0 4.625E-11											
43.0 2.595E-11											
44.0 1.453E-11											
45.0 8.087E-12											
46.0 4.502E-12											
47.0 2.537E-12											
48.0 1.407E-12											
49.0 7.826E-13											
50.0 4.364E-13											

DATE 03/04/77											
LASER LINE 2030.4082											
MODEL: MIDLATTITUDE SUMMER											
NALFAZ 3.000, ETA= 1.770											
3 2 12											
H2O 0											
CO 0											
ALT. 0.0											
TOTAL 1.635E-1											
1.0 1.635E-1											
2.0 8.175E-2											
3.0 4.088E-2											
4.0 2.044E-2											
5.0 1.022E-2											
6.0 5.111E-3											
7.0 2.556E-3											
8.0 1.278E-3											
9.0 6.390E-4											
10.0 3.195E-4											
11.0 1.598E-4											
12.0 7.990E-5											
13.0 3.995E-5											
14.0 1.998E-5											
15.0 9.990E-6											
16.0 4.995E-6											
17.0 2.498E-6											
18.0 1.249E-6											
19.0 6.245E-7											
20.0 3.123E-7											
21.0 1.561E-7											
22.0 7.805E-8											
23.0 3.903E-8											
24.0 1.952E-8											
25.0 9.760E-9											
26.0 4.880E-9											
27.0 2.440E-9											
28.0 1.220E-9											
29.0 6.100E-10											
30.0 3.050E-10											
31.0 1.525E-10											
32.0 7.625E-11											
33.0 3.813E-11											
34.0 1.906E-11											
35.0 9.530E-12											
36.0 4.765E-12											
37.0 2.383E-12											
38.0 1.191E-12											
39.0 5.955E-13											
40.0 2.978E-13											
41.0 1.489E-13											
42.0 7.445E-14											
43.0 3.723E-14											
44.0 1.861E-14											
45.0 9.305E-15											
46.0 4.653E-15											
47.0 2.326E-15											
48.0 1.163E-15											
49.0 5.815E-16											
50.0 2.908E-16											

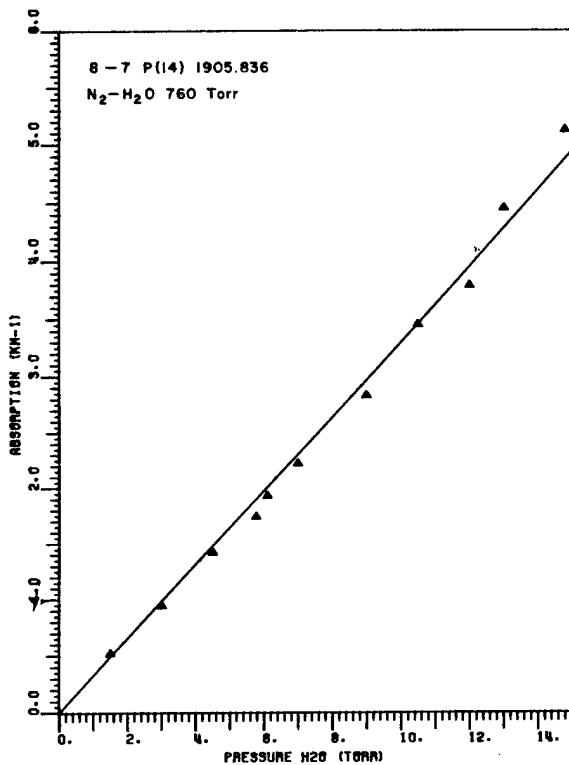
Figure 26. Calculated CO laser absorption coefficients for the mid-latitude summer model.



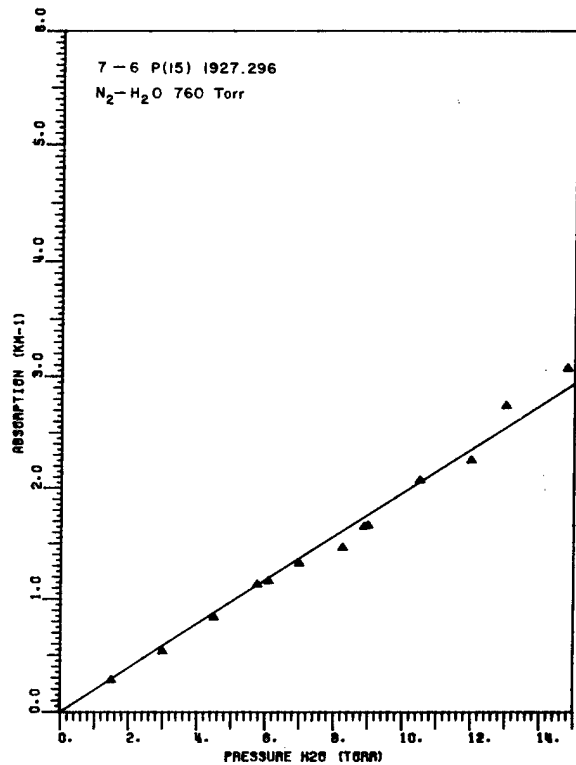
a



b

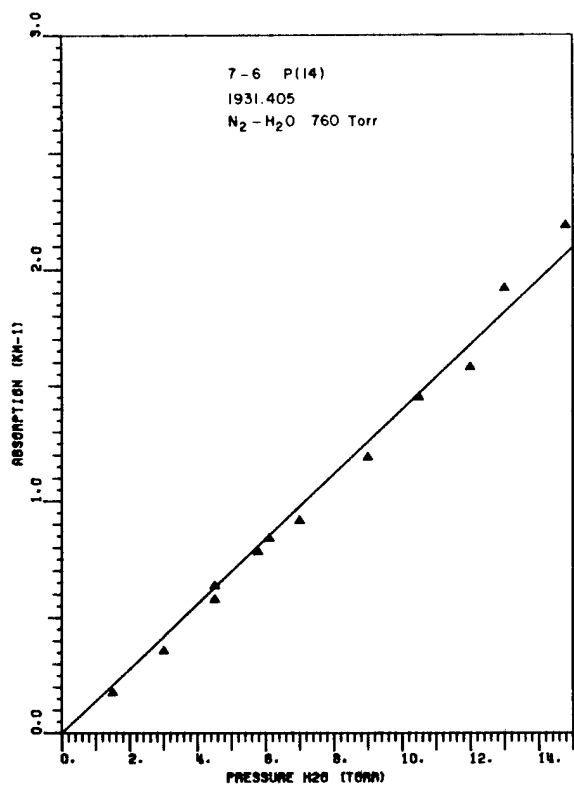


c

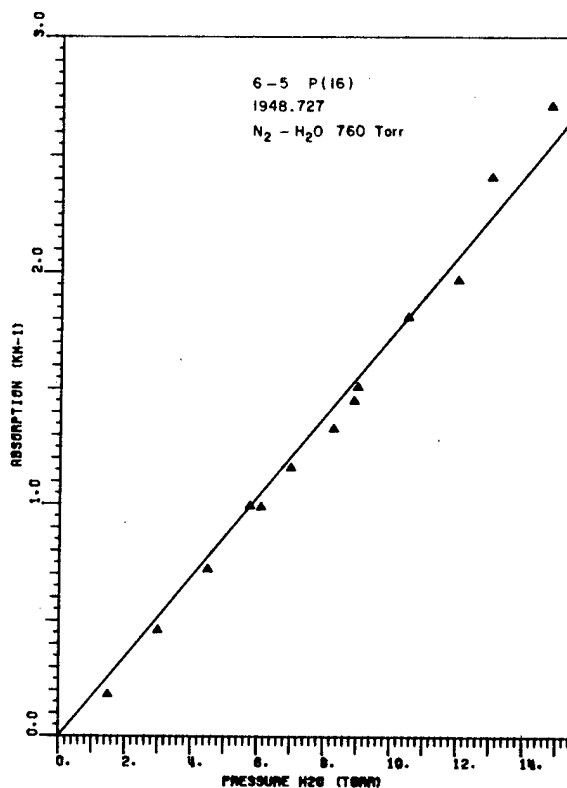


d

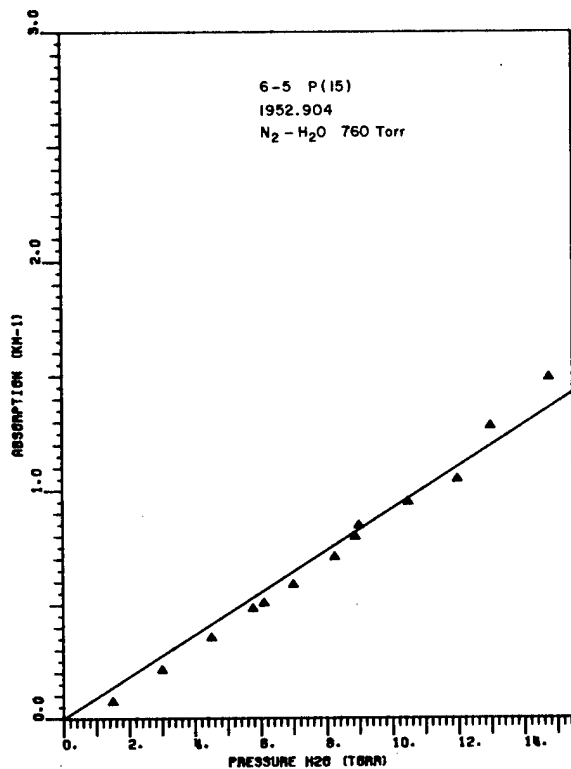
Figure 30. 1973 measurements of CO laser absorption by water vapor with linear least square fit.



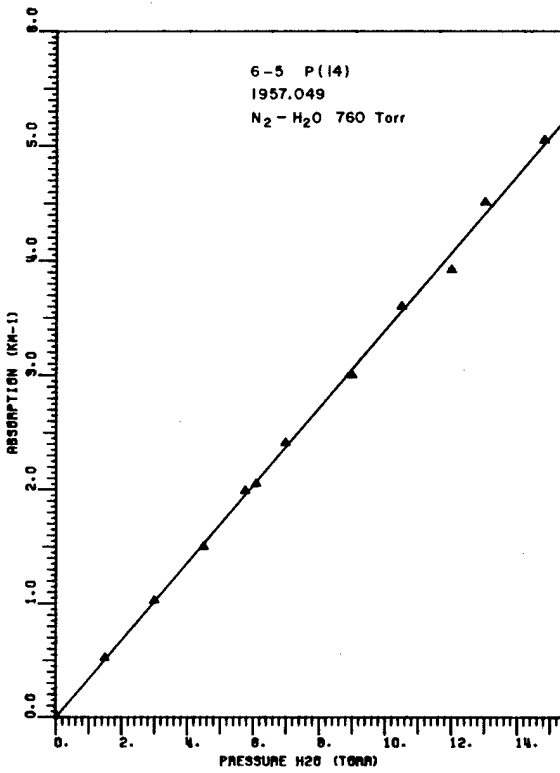
a



b

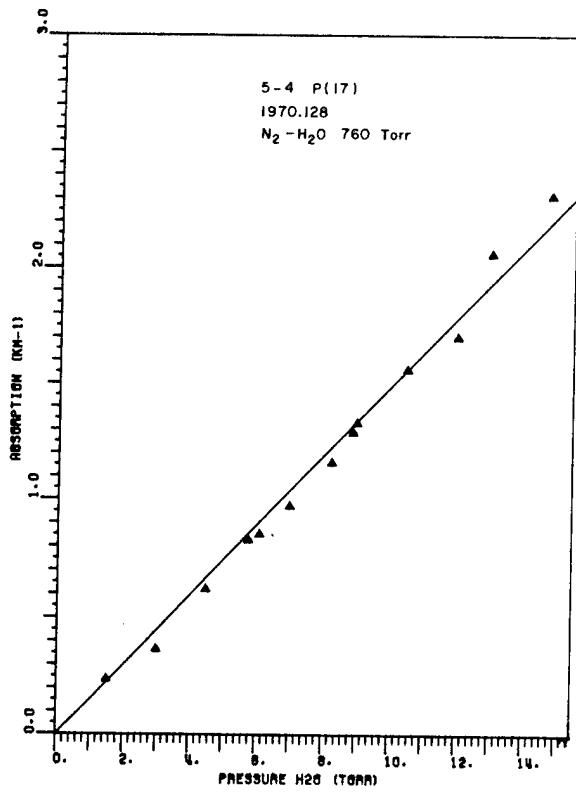


c

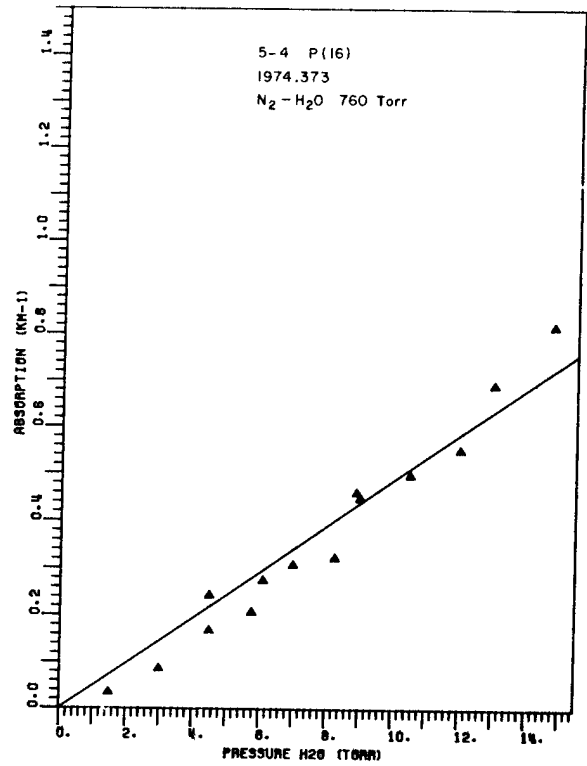


d

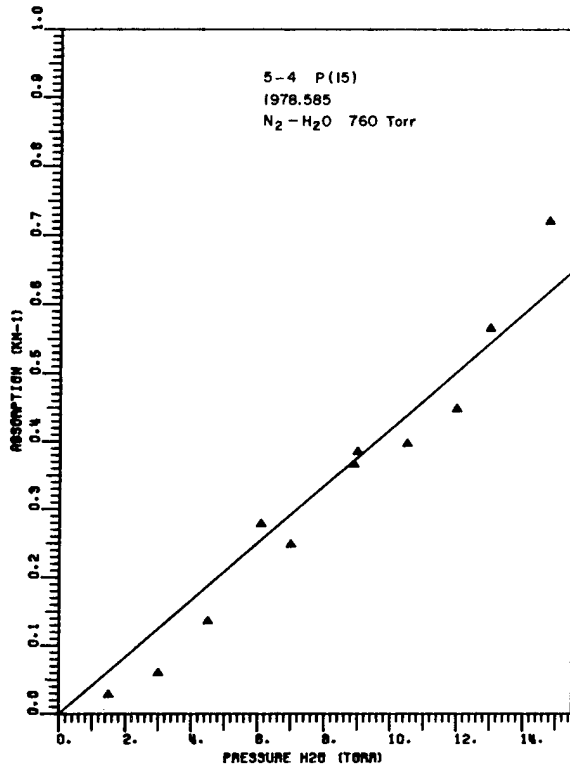
Figure 31. 1973 measurements of CO laser absorption by water vapor with linear least square fit.



a



b



c

Figure 32. 1973 measurements of CO laser absorption by water vapor with linear least square fit.

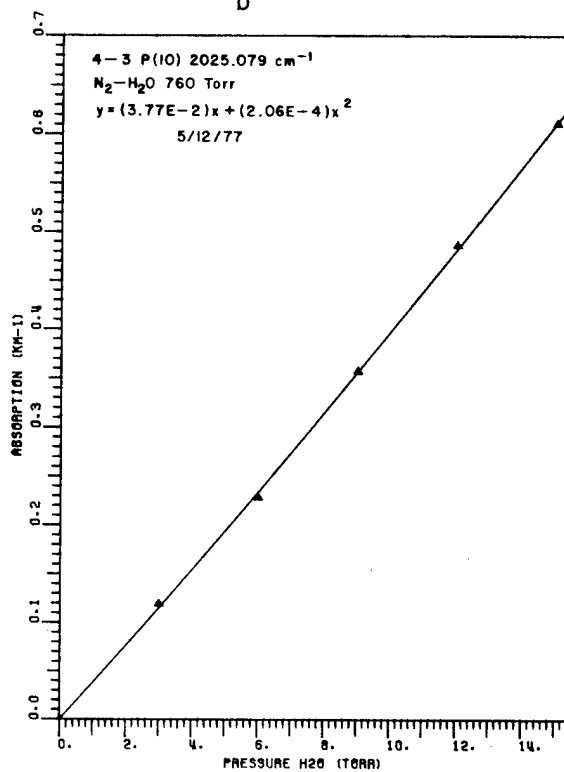
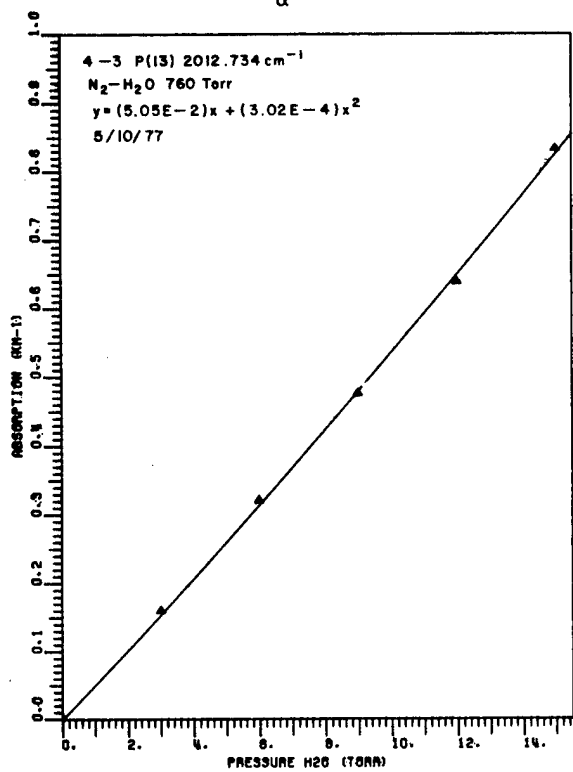
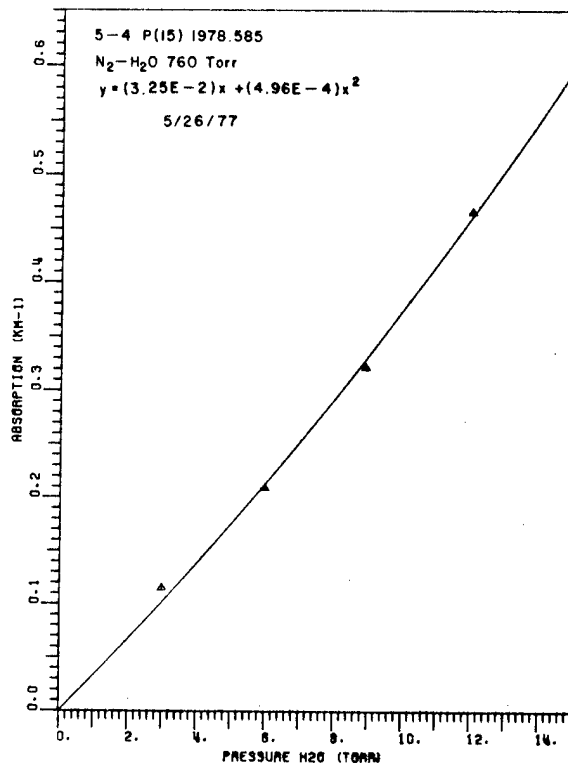
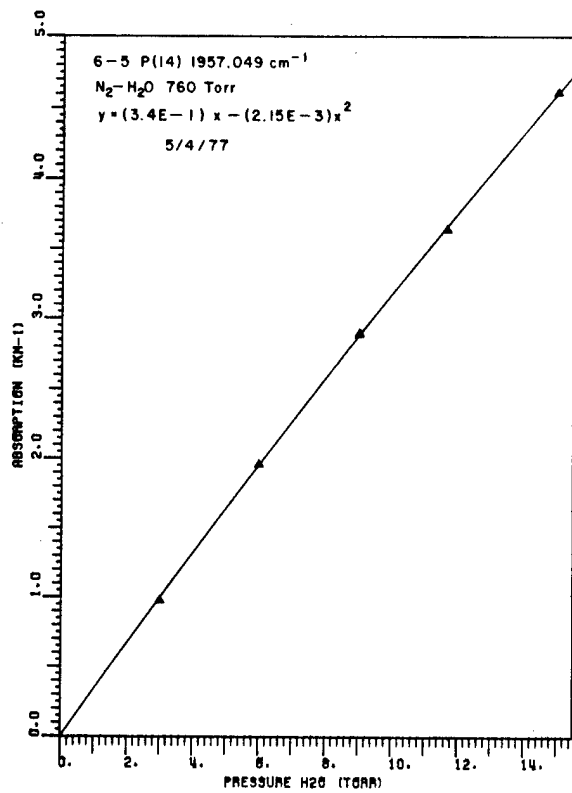


Figure 33. Measurements (1977) of CO laser absorption by water vapor for 6-5 P(14), 5-4 P(15), 4-3 P(13) and 4-3 P(10) lines.

SECTION IV
ISOTOPE CO₂ LASER TRANSMITTANCE CALCULATIONS

The spectral range of CO₂ lasers can be extended by the use of rare isotopes of CO₂ as the laser operating medium [8-10]. Determination of the laser line frequencies for various isotopes has been made to better than 0.0001 cm⁻¹ by Freed et al [11]. These lasers provide new frequencies with which to probe the atmosphere.

In a previous report [12], the attenuation of CO₂ isotope laser radiation by ground level paths of water vapor was presented. The computations were performed for the P(30) to R(30) transitions of the 636, 828, and 838 isotopes. In this preliminary study, no contribution by the water vapor continuum was included.

We have recently calculated the atmospheric attenuation of these same isotopic laser lines along horizontal paths from sea level to 50 km; the major contributors to this attenuation are carbon dioxide, ozone, and water vapor. Figure 34a-c shows the absorption coefficient in km⁻¹ for each of these molecules at three laser frequencies. The contribution of the water vapor continuum is also given. Figure 34b lists the absorption coefficients at the frequency of the P(20) transition of the common CO₂ isotope. Figures 34a and 34c list the absorption coefficients for isotopic variations having frequencies closest to the P(20) line.

Figure 35 shows the improvement in atmospheric transmittance which can be realized by selecting a laser transition in a rare isotope of CO₂. The total absorption coefficient is plotted as a function of altitude for the P(20) transition of the common isotope and for the R(24) transition of the 838 isotope. These lines are separated by 0.09 cm⁻¹. The calculated attenuation of the P(20) line is compared with a calculation by McClatchey et al. [13] and the slight deviation is probably caused by differences in the water vapor continuum calculation. The carbon dioxide contribution to this total absorption is in general agreement with work done earlier by P.K.L. Yin and R. K. Long [14].

The water vapor continuum was calculated from a curve fit by Roberts [15] to data measured by Burch [16]. The absorption coefficient can be written as

$$k(\nu) = C_s^0(\nu) w_{H_2O} [P_{H_2O} + \gamma(P-P_{H_2O})] \quad (5)$$

where w_{H_2O} is the number density of water molecules in units of

molecules \cdot cm⁻³, P_{H_2O} is the partial pressure of water vapor in atmospheres, P is the total pressure in atmospheres, $C_S^0(\nu)$ is the self-broadening coefficient at 296 K, and γ is the ratio of foreign-broadening to self-broadening. Roberts fit the function $C_S^0(\nu)$ to a form

$$C_S^0(\nu) = a + b \exp(-\sigma\nu) \quad (6)$$

where $a = 1.25 \times 10^{-22}$ cm² molecule⁻¹ atm⁻¹

$b = 1.67 \times 10^{-19}$ cm² molecule⁻¹ atm⁻¹

$\sigma = 7.87 \times 10^{-3}$ cm

Equation (5) was incorporated into the main program to calculate the 10 μ m water vapor continuum. $C_S^0(\nu)$ was taken from Equation (6) and γ was set to 0.005. There is some question as to the proper value of γ . Many workers feel that a value of 0.002 may be better.

The temperature dependence of $C_S^0(\nu)$ was also taken from a curve fit by Roberts.

$$C_S(\nu, T) = C_S^0(\nu, 296) \exp(1638 \left(\frac{1}{T} - \frac{1}{296} \right)) \quad (7)$$

This equation fits data taken by Burch at elevated temperatures, and the fit was assumed to hold at temperatures below 296 K.

DATE 06/02/77
LASER LINE 944.195
MODEL: MIDLATITUDE SUMMER 0 0
NAIFAM 30.000, ETA= 2.000

ALT.	H2O	CO2	O3	TOTAL	H2O C	CO2 C	O3 C	TOTAL C
0.0	7.218E-3	3.243E-2	3.448E-8	2.576E-1	2.972E-1	1.043E-2	8.251E-2	3.974E-8
1.0	3.741E-3	2.588E-2	2.742E-8	1.599E-1	1.303E-1	5.483E-3	7.553E-2	3.168E-8
2.0	1.790E-3	1.995E-2	2.119E-8	8.510E-2	6.316E-2	2.058E-3	6.743E-2	2.452E-8
3.0	7.257E-4	1.476E-2	1.619E-8	4.208E-2	3.426E-2	1.585E-3	5.073E-2	1.875E-8
4.0	3.020E-4	1.075E-2	1.228E-8	2.342E-2	1.936E-2	1.140E-3	3.642E-2	1.422E-8
5.0	1.140E-4	7.683E-3	9.211E-9	1.319E-2	8.430E-3	7.675E-4	2.572E-2	1.009E-8
6.0	4.100E-5	5.366E-3	6.722E-9	8.430E-3	5.389E-3	5.389E-4	1.875E-2	7.387E-9
7.0	1.465E-5	3.866E-3	4.847E-9	5.714E-3	3.866E-3	3.866E-4	1.367E-2	5.387E-9
8.0	5.070E-6	2.817E-3	3.480E-9	4.142E-3	2.817E-3	2.817E-4	1.009E-2	3.951E-9
9.0	1.818E-6	1.956E-3	2.488E-9	2.988E-3	1.956E-3	1.956E-4	7.387E-3	2.817E-9
10.0	6.113E-7	1.402E-3	1.898E-9	2.136E-3	1.402E-3	1.402E-4	5.387E-3	2.136E-9
11.0	2.113E-7	1.022E-3	1.366E-9	1.514E-3	1.022E-3	1.022E-4	3.951E-3	1.514E-9
12.0	7.450E-8	7.345E-4	1.017E-9	1.088E-3	7.345E-4	7.345E-5	2.817E-3	1.088E-9
13.0	2.584E-8	5.345E-4	7.345E-10	7.654E-4	5.345E-4	5.345E-5	2.136E-3	7.654E-10
14.0	8.899E-9	3.939E-4	5.345E-10	5.624E-4	3.939E-4	3.939E-5	1.514E-3	5.624E-10
15.0	3.020E-9	2.817E-4	3.939E-10	4.048E-4	2.817E-4	2.817E-5	1.140E-3	4.048E-10
16.0	1.075E-9	1.995E-4	2.817E-10	2.988E-4	1.995E-4	1.995E-5	8.430E-4	2.988E-10
17.0	3.741E-10	1.476E-4	1.995E-10	2.136E-4	1.476E-4	1.476E-5	6.316E-4	2.136E-10
18.0	1.476E-10	1.075E-4	1.476E-10	1.514E-4	1.075E-4	1.075E-5	4.642E-4	1.514E-10
19.0	5.345E-11	7.683E-5	1.075E-10	1.088E-4	7.683E-5	7.683E-6	3.426E-4	1.088E-10
20.0	1.956E-11	5.345E-5	7.683E-11	7.683E-5	5.345E-5	5.345E-6	2.572E-4	7.683E-11
21.0	6.810E-12	3.939E-5	5.345E-11	5.624E-5	3.939E-5	3.939E-6	1.875E-4	5.624E-11
22.0	2.345E-12	2.817E-5	3.939E-11	4.048E-5	2.817E-5	2.817E-6	1.367E-4	4.048E-11
23.0	8.430E-13	1.995E-5	2.817E-11	2.988E-5	1.995E-5	1.995E-6	1.009E-4	2.988E-11
24.0	2.988E-13	1.476E-5	1.995E-11	2.136E-5	1.476E-5	1.476E-6	7.387E-5	2.136E-11
25.0	1.088E-13	1.075E-5	1.476E-11	1.514E-5	1.075E-5	1.075E-6	5.387E-5	1.514E-11
30.0	2.817E-14	7.387E-6	1.075E-11	1.088E-5	7.387E-6	7.387E-7	3.951E-5	1.088E-11
35.0	6.128E-15	5.345E-6	7.387E-12	7.683E-6	5.345E-6	5.345E-7	2.817E-5	7.683E-12
40.0	1.465E-15	3.866E-6	5.345E-12	5.714E-6	3.866E-6	3.866E-7	2.136E-5	5.714E-12
45.0	5.070E-16	2.817E-6	3.866E-12	4.142E-6	2.817E-6	2.817E-7	1.514E-5	4.142E-12
50.0	1.818E-16	1.956E-6	2.817E-12	2.988E-6	1.956E-6	1.956E-7	1.140E-5	2.988E-12

DATE 06/02/77
LASER LINE 944.195
MODEL: MIDLATITUDE SUMMER 0 0
NAIFAM 30.000, ETA= 2.000

ALT.	H2O	CO2	O3	TOTAL	H2O C	CO2 C	O3 C	TOTAL C
0.0	7.218E-3	3.243E-2	3.448E-8	2.576E-1	2.972E-1	1.043E-2	8.251E-2	3.974E-8
1.0	3.741E-3	2.588E-2	2.742E-8	1.599E-1	1.303E-1	5.483E-3	7.553E-2	3.168E-8
2.0	1.790E-3	1.995E-2	2.119E-8	8.510E-2	6.316E-2	2.058E-3	6.743E-2	2.452E-8
3.0	7.257E-4	1.476E-2	1.619E-8	4.208E-2	3.426E-2	1.585E-3	5.073E-2	1.875E-8
4.0	3.020E-4	1.075E-2	1.228E-8	2.342E-2	1.936E-2	1.140E-3	3.642E-2	1.422E-8
5.0	1.140E-4	7.683E-3	9.211E-9	1.319E-2	8.430E-3	7.675E-4	2.572E-2	1.009E-8
6.0	4.100E-5	5.366E-3	6.722E-9	8.430E-3	5.389E-3	5.389E-4	1.875E-2	7.387E-9
7.0	1.465E-5	3.866E-3	4.847E-9	5.714E-3	3.866E-3	3.866E-4	1.367E-2	5.387E-9
8.0	5.070E-6	2.817E-3	3.480E-9	4.142E-3	2.817E-3	2.817E-4	1.009E-2	3.951E-9
9.0	1.818E-6	1.956E-3	2.488E-9	2.988E-3	1.956E-3	1.956E-4	7.387E-3	2.817E-9
10.0	6.113E-7	1.402E-3	1.898E-9	2.136E-3	1.402E-3	1.402E-4	5.387E-3	2.136E-9
11.0	2.113E-7	1.022E-3	1.366E-9	1.514E-3	1.022E-3	1.022E-4	3.951E-3	1.514E-9
12.0	7.450E-8	7.345E-4	1.017E-9	1.088E-3	7.345E-4	7.345E-5	2.817E-3	1.088E-9
13.0	2.584E-8	5.345E-4	7.345E-10	7.654E-4	5.345E-4	5.345E-5	2.136E-3	7.654E-10
14.0	8.899E-9	3.939E-4	5.345E-10	5.624E-4	3.939E-4	3.939E-5	1.514E-3	5.624E-10
15.0	3.020E-9	2.817E-4	3.939E-10	4.048E-4	2.817E-4	2.817E-5	1.140E-3	4.048E-10
16.0	1.075E-9	1.995E-4	2.817E-10	2.988E-4	1.995E-4	1.995E-5	8.430E-4	2.988E-10
17.0	3.741E-10	1.476E-4	1.995E-10	2.136E-4	1.476E-4	1.476E-5	6.316E-4	2.136E-10
18.0	1.476E-10	1.075E-4	1.476E-10	1.514E-4	1.075E-4	1.075E-5	4.642E-4	1.514E-10
19.0	5.345E-11	7.683E-5	1.075E-10	1.088E-4	7.683E-5	7.683E-6	3.426E-4	1.088E-10
20.0	1.956E-11	5.345E-5	7.683E-11	7.683E-5	5.345E-5	5.345E-6	2.572E-4	7.683E-11
21.0	6.810E-12	3.939E-5	5.345E-11	5.624E-5	3.939E-5	3.939E-6	1.875E-4	5.624E-11
22.0	2.345E-12	2.817E-5	3.939E-11	4.048E-5	2.817E-5	2.817E-6	1.367E-4	4.048E-11
23.0	8.430E-13	1.995E-5	2.817E-11	2.988E-5	1.995E-5	1.995E-6	1.009E-4	2.988E-11
24.0	2.988E-13	1.476E-5	1.995E-11	2.136E-5	1.476E-5	1.476E-6	7.387E-5	2.136E-11
25.0	1.088E-13	1.075E-5	1.476E-11	1.514E-5	1.075E-5	1.075E-6	5.387E-5	1.514E-11
30.0	2.817E-14	7.387E-6	1.075E-11	1.088E-5	7.387E-6	7.387E-7	3.951E-5	1.088E-11
35.0	6.128E-15	5.345E-6	7.387E-12	7.683E-6	5.345E-6	5.345E-7	2.817E-5	7.683E-12
40.0	1.465E-15	3.866E-6	5.345E-12	5.714E-6	3.866E-6	3.866E-7	2.136E-5	5.714E-12
45.0	5.070E-16	2.817E-6	3.866E-12	4.142E-6	2.817E-6	2.817E-7	1.514E-5	4.142E-12
50.0	1.818E-16	1.956E-6	2.817E-12	2.988E-6	1.956E-6	1.956E-7	1.140E-5	2.988E-12

Figure 34. Calculated absorption coefficients for mid-latitude summer model for three isotope CO2 laser lines. (a) 838 R(24), 944.103 cm⁻¹, (b) 626 P(20), 944.195 cm⁻¹, and (c) 828 P(28), 944.997 cm⁻¹.

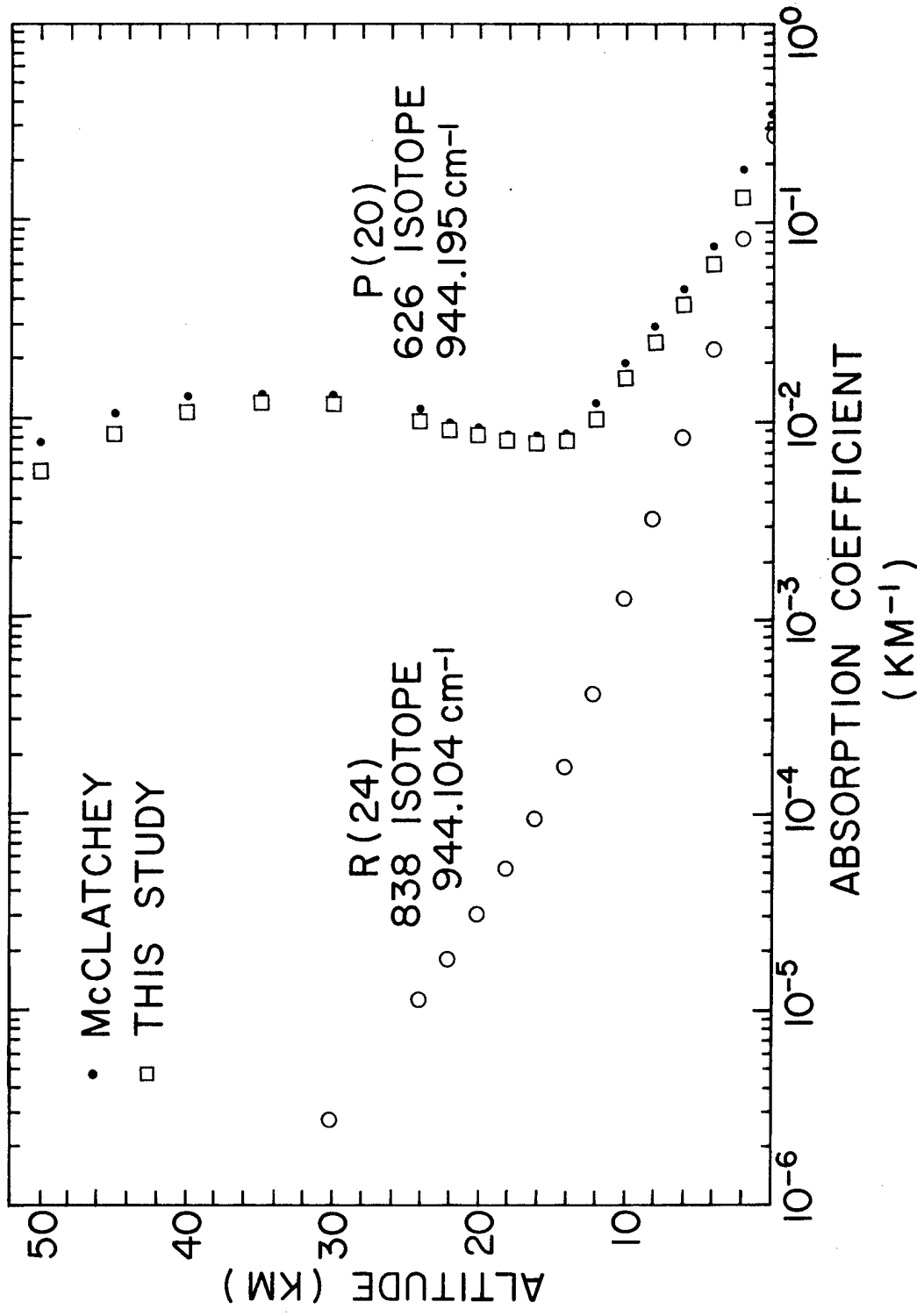


Figure 35. Comparison of calculated absorption coefficient for 626 P(20) and 838 R(24) Laser Lines.

SECTION V
OZONE SPECTROSCOPY NEAR 5 μm

Ozone spectra are very complex with many closely spaced lines. In the case of overlapping bands the situation becomes even worse. Because of this, it was decided early on that we should try for the best possible resolution. High resolution would help in separating close lines and in identifying predicted lines by increasing line position precision. We therefore are using our highest resolution grating. Unfortunately there is no gas known to us which is well suited to use in the overlapping order technique of line calibration.

There is however on our spectrometer a very precise grating angle indicator capable of measuring angle differences corresponding to less than 0.0025 cm^{-1} . It was hoped that we could calibrate the grating position with well known CO lines in the $5\ \mu\text{m}$ region and then use the position calibration to measure O₃ line positions. To do this would require unknown degrees of stability in the optical alignment as well as the pressure inside the spectrometer and the temperature of the grating.

We first aligned the spectrometer for resolution of better than 0.05 cm^{-1} determined by measuring the full width at half maximum of narrow CO lines. We next experimented with different collection parameters (slit widths, time constants, scan speed, etc.) in order to determine the values giving the best spectra. After some initial difficulties we collected a series of CO spectra to determine system stability. It was found to be stable only over a matter of hours. Consequently we will calibrate the spectra with CO lines and previously determined strong ozone lines. We have already done this for several spectra. A preliminary comparison of our results with those of Maki [1] give agreement of $\pm 0.005\text{ cm}^{-1}$.

Figure 36 is a portion of a preliminary ozone spectrum taken while conditioning the cell to hold ozone. It was calibrated by using the two CO lines indicated on the spectrum which were scanned at a much lower ozone concentration an hour before. This region should be compared to Figure 5 of the proposal for this work which shows the same region as computed from the AFGL line listing data. While our spectra includes lines of the $2\nu_3$ band as well as the $\nu_1+\nu_3$ band shown in Figure 5 of the proposal, a comparison with the data in the paper by Maki [17] shows that the line lying on the 2-1 CO laser line was identified by Maki as being the P(29,1) line. The line position determined from our spectrum is rough due to the fact that we calibrated with only two CO lines. Our value is 2082.257 cm^{-1} compared to 2082.2586 cm^{-1} by Maki.

Early in April 1977 we cooled the cell down for the first time. By simply laying blocks of dry ice inside the tub the cell reached -0°C in about 3 days. The heat leak was $2.6 \text{ watts}/^{\circ}\text{C}$ which is very close to the expected value of $2.2 \text{ watts}/^{\circ}\text{C}$ calculated by 6" of styrofoam. The only major problem encountered during the trial was a failure of the silicone O-rings around the windows at temperatures below -40°C . We are currently trying different seal types to correct this problem.

We have collected seven high resolution ozone spectra at room temperature which will be compared with Maki's results. Some analysis of these has already been done. Four of these spectra were collected while simultaneously monitoring the ozone concentration with a UV spectrometer and a low pressure Hg lamp. These spectra can thus be used to determine line strengths.

So far, we have taken high resolution infrared spectra of the $\nu_1+\nu_2$ band of ozone, with wavenumbers between 2104.6 cm^{-1} and 2064.2 cm^{-1} at room temperature and low pressure (less than 40 Torr). These spectra can be compared with Maki's observed data in order to check the resolution and precision of our experimental data before we take any spectra of the $2\nu_3$ band of ozone. More than 400 lines of ozone were observed in this region, and about 18 of these lines were not listed in Maki's paper.

Table I lists our observed lines and Maki's between 2086.5 cm^{-1} and 2081.3 cm^{-1} . From the differences of these two data sets (shown in Table I) we can see our values for each line position are slightly higher than Maki's. This systematic error is because our values for the CO calibration lines taken from Rao et al [18] are slightly higher than those used by Maki as indicated in Maki's paper. Most of the differences are less than 0.008 cm^{-1} . Those lines whose differences are higher than 0.01 cm^{-1} are weak transition lines. Our values listed in Table I were obtained merely from one of our spectra. We should be able to get higher precision especially for those weak transition lines later when we measure several spectra at different temperature and pressure.

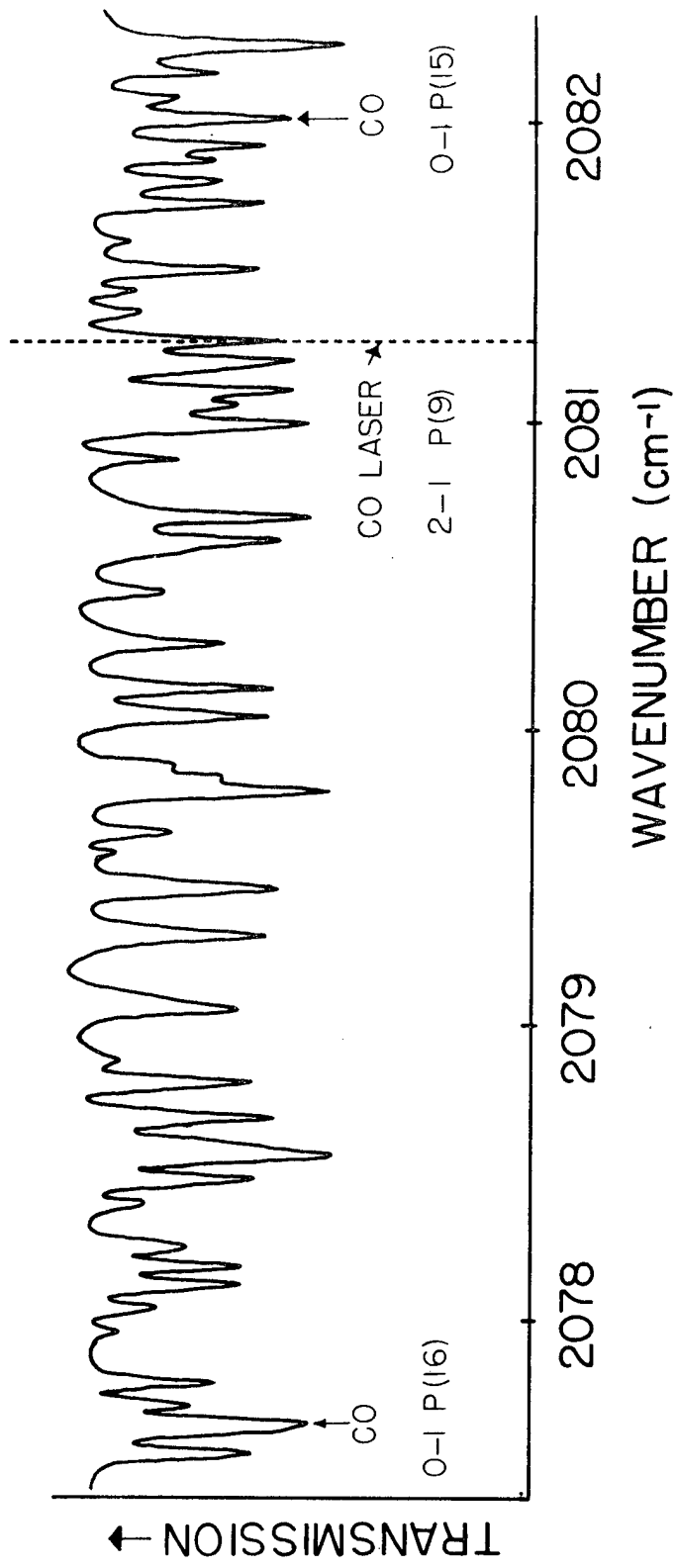


Figure 36. Ozone spectrum, room temperature.

Table I

Present Observed(cm^{-1})	Maki's Observed(cm^{-1})	(Present - Maki's) Observed(cm^{-1})
2086.4731	2086.4717	0.0014
2086.4345	2086.4300	-0.0045
2086.3234 CO-P(14)	2086.3219 CO-O(14)	0.0015
2086.2540	2086.2491	0.0049
2086.1350	2086.1287	0.0063
2086.0578	2086.0508	0.0070
2086.0290	2086.0237	0.0053
2085.8595	2085.8534	0.0061
2085.7748	2085.7678	0.0070
2085.7058	2085.7066	-0.0008
2085.6325	2085.6252	0.0073
2085.5146	2085.5112	0.0034
2085.4191	2085.4141	0.0050
2085.3517	2085.3405	0.0067
2085.0912	2085.0824	0.0088
2085.0043	2084.9970	0.0073
2084.9207	2084.9134	0.0073
2084.8480	2084.8405	0.0075
2084.6880	2084.6806	0.0074
2084.6158	2084.6088	0.0070
2084.4857	2084.4835	0.0022
2084.4211	2084.4135	0.0076
2084.3381	2084.3280	0.0101
2084.2102	2084.2017	0.0085
2084.1034	2084.0977	0.0057
2084.0454	2084.0385	0.0060
2083.9093	2083.9018	0.0075
2083.6687	2083.6594	0.0093
2083.5945	2083.5890	0.0050
2083.4525	2083.4483	0.0042
2083.3447	2083.3346	0.0101
2083.2825	2083.1855	0.0970
2083.1260	2083.1240	0.0020
2083.0426	2083.0357	0.0069
2082.8206	2082.8187	0.0019
2082.7162	2082.7072	0.0090
2082.5960	2082.5891	0.0069
2082.4635	2082.4623	0.0012
2082.2584	2082.2561	0.0023
2082.1670	2082.1631	0.0039
2082.0799	2082.0728	0.0071
2082.0037 CO-P(15)	2082.0033 CO-P(15)	0.0004
2081.9183	2081.9119	0.0064
2081.8718	2081.8680	0.0038
2081.7955	2081.7908	0.0047
2081.7231	2081.7161	0.0070
2081.6036	2081.6010	0.0026
2081.5053	2081.4971	0.0082
2081.4399	2081.4305	0.0094
2081.3664	2081.3560	0.0104

SECTION VI
MISCELLANEOUS TOPICS

A. Modification of Sylvania CO₂ Laser

The modification of a Sylvania Model 948 CO₂ laser to a single line, grating tunable laser has been successfully completed. The original plan [19], which called for the retro-fitting of a grating mount and associated optics on the Sylvania laser head, however, was not successful. Severe stability problems were observed in this operation of the laser using the original scheme. The source of this difficulty was traced to a flexing of the aluminum base plate on which the laser tube and optics were mounted. As supplied by the manufacturer, the laser optics (an internal flat output mirror and external gold coated spherical mirror) are mounted on the plasma tube; hence problems associated with the rigidity of the base are minimized. Our first design however required that the spherical mirror be removed and re-mounted together with the grating optics on the 1/4" aluminum base plate. This situation permitted relative motion between the internal output mirror on the plasma tube and the other components of the resonant cavity which led to an unstable condition for laser operation.

To correct this problem the laser table was remounted on a 3" thick limestone slab, 12" wide and 5' long. This base, which is nearly 2' longer than the original, also permitted illumination of a plane "turning" mirror which was required in the first design. A schematic diagram of the revised laser optics is shown in Figure 37. For this type of resonator the stability condition (not to be confused with the mechanical problems discussed earlier) can be shown to be

$$0 < \left(1 - 2 \frac{L_1}{R}\right) \left(1 - 2 \frac{L_2}{R}\right) < 1$$

where the distances L_1 , L_2 are illustrated in the figure and R is the radius of curvature for the spherical mirror. For the present situation we have $L_1 = 1.1$ m, $L_2 = .3$ m and $R = 3$, hence

$$0 < .21 < 1$$

is satisfied.

An interesting aspect of this laser is introduced by the presence of the gallium arsenide flat, which serves as the output mirror, i.e., it is used as an etalon. This means that the output mirror is frequency selective and on cold start will not allow operation of many strong laser lines, among which are the P(20) and R(20) lines in the 10 μ m band. However, this etalon is temperature sensitive so that its frequency properties can be altered by heating or cooling. When this difficulty arises we have been able to easily overcome the problem by running the laser on an "operable" line near the desired

frequency to heat the output mirror and this quickly readjusting the grating for the desired laser line. Using this process we have obtained the following laser lines:

10 μm band

9 μm band

P(12) - P(36), R(8) - R(32)

P(12)-P(20); R(10)-R(34)

No strong effort has been made to find all of the operable lines.

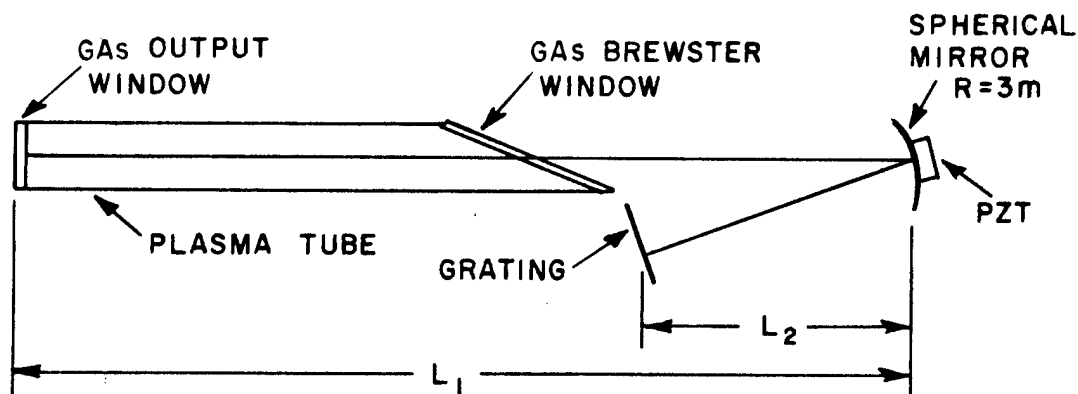
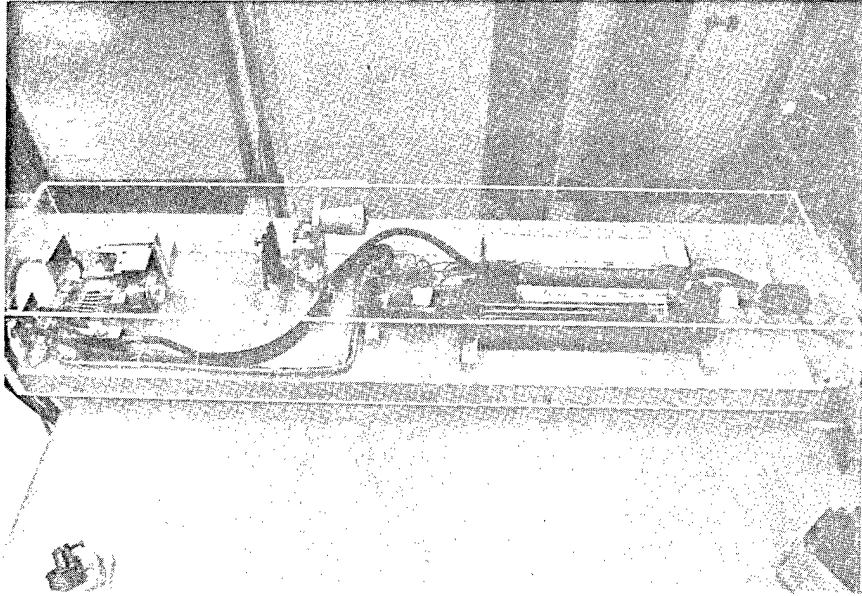
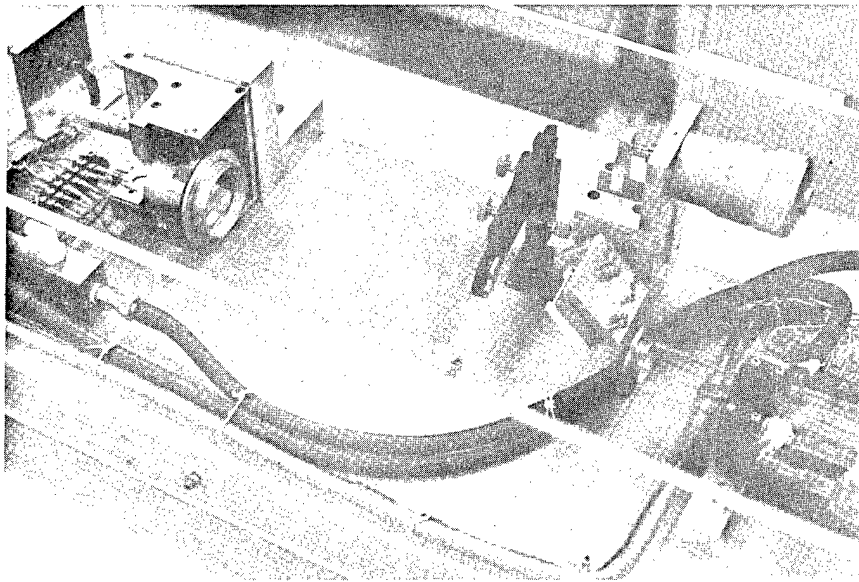


Figure 37. Schematic diagram of optics of modified Sylvania laser.

The laser operates at a nominal power of 4 watts on the P(20) line of the 10 μm band. Because of the large power intensities within the optical cavity, approximately 1000 w/cm², we are using an original grating ruled with 150 lines/mm and blazed at 8.6 μm . This grating was chosen for its relatively large angular dispersion which permits precise tuning of the desired line. To assure maximum stability the laser head has been enclosed in a 3/8" thick plexiglass box with one small covered opening that permits adjustment of the grating micrometer. Also the laser has been connected to the electronic frequency stabilizer which we have successfully used in several other instruments. Thus far, we have found the laser to be a dependable and stable radiation source. A picture of the completed laser is shown in Figures 38a and 38b.



(a)



(b)

Figure 38. Photograph of the modified CO₂ laser.

B. CW HF-DF Laser System

First operation of the Hinchey-style [20] continuous-wave HF-DF laser was made using an 80% broadband reflective germanium output mirror with a 10-m radius of curvature and a first-surface plane mirror. Cavity length is 29 cm, with the region of active gain about 10 cm. CaF₂ windows, mounted at the Brewster angle, were used.

TEM₀₀ lasing was achieved using the following composition of gases; as measured by their partial pressure components within the mixing region: SF₆=4.5 mbar, O₂=6.5 mbar, H₂=2.5 mbar, He (for window purge) =1.0 mbar. Discharge voltage, with 350 K Ω of ballast resistance on each of the twelve electrodes comprising the cathode, was 14.2 kv. Discharge current, with the gas composition listed above, was 98 mA.

It was soon observed that variation in the gas mixture caused great changes in the V-I characteristics of the discharge although the effect on laser output was comparatively small. For this reason, laser power output was monitored while the component of a single gas was varied by small increments, with care being taken to keep the discharge current somewhere between 95 and 100 mA.

In the process, it was observed that if discharge current was increased from this value for a given gas composition, laser output would drop by a comparable factor. Since the discharge would not sustain itself below 90 mA current with the ballast resistance used, the value of 98 mA was taken to be a reasonable point from which to attempt to optimize power output. Checking of a wide range of gas mixture indicated that no small variation of a single gas caused any abrupt change in output characteristics, and that the relative components listed above were close to an optimum mix for multiline lasing.

The orientation of the output mirror was observed to be by far the most sensitive operating parameter in maximizing power output and the positioning of the optical cavity downstream from the mixing point, previously thought to be quite critical, did not turn out to be so. Lasing was originally observed with the optical settings very close to those arrived at by alignment with a He-Ne laser, with the optical cavity being about 1.5 mm downstream from the mixing point. At this time it was observed that very slight adjustments in the elevation or azimuthal position of the mirror, or even the pressure of a finger on the mirror mount, was enough to either greatly increase the power output or, by the same token, eliminate it. Moving the cavity up and down stream from this point has a similar effect, but less pronounced. In the course of varying the position of the output mirror, laser action was lost and regained several times, at points from 1.5 mm upstream to 3 mm downstream of the mixing point, with comparable power outputs. Once a fairly strong (>25 mW) power output was achieved, a tendency was noticed for the laser to "self-maximize",

where the power would rise steadily for 10 seconds or so in the absence of any manual adjustment. The time constant of the thermopile used to measure power was about 2 seconds, and so is not itself an explanation for this phenomenon.

Through a combination of gingerly tweaking and touching of the output mirror, a power out of .33 W, multiline was eventually realized. Power output, in the absence of any variation in operating conditions, was observed to be quite stable, varying no more than 10% over 30 minutes of operation, although this does not take into account fluctuations of duration appreciably smaller than the time constant of the thermopile.

After several hours of operation, a light deposit of matter was noticed on the rear window. This may have resulted from impurities in the He purge line, or from sulfur depositing from the discharge. The deposit was a circular spot about in the center of the window, 5 mm in diameter and was detected when it became evident that maximum achievable power out was lessening over the course of time. Both windows have since been cleaned and re-mounted.

Hinchen's report on the operating characteristics of this laser system [20] quotes a gain coefficient of $.033 \text{ cm}^{-1}$, or about 30% per pass. Since the output mirror is 80% reflective, the possibility of over-coupling must be considered. Experiments are currently under way to determine if this condition exists.

Single-line DF lasing using the Hinchen style continuous wave HF-DF laser system has been achieved using a 98% reflecting ZnSe mirror with a 2m radius of curvature, and a 300 line/mm diffraction grating blazed at 3 microns. Lasing was observed on a total of 18 lines covering the 3-2, 2-1, 1-0 vibrational bands. Operating conditions and gas mixtures were the same as indicated in the operation on multiline HF with the exception of substitution of deuterium for hydrogen. The strongest lines observed were P5 thru P11 on the 2-1 vibrational band. Positive identification of these lines was made using a spectrometer specifically designed for measurement in the DF spectral region (3.7-3.9 μm). Weaker lines too low in intensity to be observed on the spectrometer detection screen ($\sim 40 \text{ mW}$) were identified by measuring the shift in micrometer setting of the grating between observed transitions to derive a ratio between shift in setting and shift in wavenumber (a relationship which, due to the grating mount design, was known to be nearly linear) and then extrapolating the wavenumber of an observed line and cross-checking it with tabulated values for various vibrational-rotational transitions. A table of observed lines and relative strengths is given below:

Table II

<u>Transitions</u>	<u>Wavenumber</u>	<u>Peak Power (mW)</u>	<u>Micrometer Setting</u>
1-0 P(5)	2792.434	12	4.541
1-0 P(6)	2767.968	24	4.683
1-0 P(7)	2742.998	36	4.829
2-1 P(4)	2727.309	18	4.920
1-0 P(8)	2717.539	31	4.980
2-1 P(5)	2703.999	40	5.062
1-0 P(9)	2691.607	28	5.134
2-1 P(6)	2680.179	59	5.206
1-0 P(10)	2665.219	25	5.292
2-1 P(7)	2655.863	72	5.364
2-1 P(8)	2631.068	104	5.507
2-1 P(9)	2605.807	118	5.680
2-1 P(10)	2580.097	92	5.895
3-2 P(7)	2570.522	10	5.916
2-1 P(11)	2553.953	46	6.027
3-2 P(8)	2546.375	28	6.075
3-2 P(9)	2521.769	25	6.244
3-2 P(10)	2496.721	18	6.425

Further experimentation will include variation in gas mixing cell temperature to determine how best to enhance power output from the various lines. Attempts will also be made to improve laser stability so that experiments to determine optimum coupling of the laser for each line may be conducted.

C. Microcomputer Data Link

An Imsai microcomputer and Altair A/D converter have been implemented as a link to the laboratory time sharing system. After initial testing is completed this unit is expected to replace the SDS920 computer for data acquisition on the spectrophone and White cell experiments. This should reduce maintenance cost and increase productivity due to the ease with which the time sharing system can be programmed.

D. Fourier Transform Spectrometer

A Nicolet FTS system has now been received. The optical retardation is 20.5 cm. A dedicated minicomputer with disc storage system is included as well as complete software for spectral data manipulation. This system will be used in future White cell measurements and will provide additional information concerning cell conditions during laser transmittance measurements.

REFERENCES

- [1] RADC-TR-76-330, Part B.
- [2] RADC-TR-76-389, Section V.
- [3] RADC-TR-74-95.
- [4] AFCRL-71-0370, 1 July 1971.
- [5] T. R. Todd, et al., "Infrared Emission of $^{12}\text{C}^{16}\text{O}$, $^{13}\text{C}^{16}\text{O}$, and $^{12}\text{C}^{18}\text{O}$ ", Journal of Molecular Spectroscopy, Vol. 62, pp. 201-227, (1976).
- [6] RADC-TR-73-389.
- [7] RADC-TR-73-126.
- [8] I. Wieder and G. B. McCurdy, Phys. Rev. Lett 16, 565 (1966).
- [9] G. B. Jacobs and H. C. Bowers, J. Appl. Phys. 38, 2629 (1967).
- [10] J. C. Siddoway, J. Appl. Phys. 39, 4854 (1968).
- [11] C. Freed, A.H.M. Ross, and R. G. O'Donnell, J. Molec. Spectros 49, 439 (1974).
- [12] R. K. Long, E. K. Damon, R. J. Nordstrom, J. C. Peterson, M. E. Thomas, and J. P. Serifin, "Laser Atmospheric Absorption Studies," RADC-TR-76-389, January 1977.
- [13] R. A. McClatchey, R. W. Fenn, J.E.A. Selby, F.E. Volz, and J. S. Garing, "Optical Properties of the Atmosphere (Third Edition)", AFCRL-72-0497, August 1972.
- [14] P.K.L. Yin and R.K. Long, Appl. Opt. 7, 1551 (1968).
- [15] R. E. Roberts, L. M. Biberman, and J.E.A. Selby, "Infrared Continuum Absorption by Atmospheric Water Vapor in the 8-12 μm Window", Institute for Defense Analysis Science and Technology Division, IDA Log No. HQ 76-18059, April 1976.
- [16] D. E. Burch, Aeronutronic Publication No. U-4784, "Semi-Annual Technical Report", AFCRL Contract No. F19628-69-C-0263, January 1970.

- [17] A. G. Maki, J. Mol. Spec. 57, 416 (1975).
- [18] K. N. Rao, C.J. Humphreys, and D.H. Rank, "Wavelength Standards in the Infrared", Academic Press, New York, 1966.
- [19] RADC-TR-76-389, p. 54.
- [20] J. J. Hinchey, "Operation of a Small Single Mode Stable CW Hydrogen Fluoride Laser", United Aircraft Research Laboratories Report UAR-M135, October 15, 1973.